Reviewed Preprint
v1 • July 14, 2025
Not revised

Reviewed Preprint
v2 • September 16, 2026
Revised by authors

For correspondence:
dw657@drexel.edu

Competing interests: No competing interests declared

Funding: See page 25

Reviewing editor: Adrien Peyrache, McGill University, Canada

A cortical–hippocampal communication undergoes rebalancing after new learning

Arron F Hall, Dong V Wang

Department of Neurobiology & Anatomy, Drexel University College of Medicine, Philadelphia, United States

eLife Assessment

This **valuable** study investigates communication from the anterior cingulate cortex to the hippocampus during learning. The optogenetic evidence supporting the functional connection including the interneurons likely to be involved, is **convincing**. However, the evidence linking this pathway to learning and memory and certain aspects of the statistical interpretation remain limited. Overall, the work will be of interest to neuroscientists studying cortical-hippocampal interactions and learning and memory.

https://doi.org/10.7554/eLife.107370.2.sa2

Abstract

The brain's ability to consolidate a wide range of memories while maintaining their distinctiveness across experiences remains poorly understood. Sharp-wave ripples, neural oscillations that occur predominantly within CA1 of the hippocampus during immobility and sleep, have been shown to play a critical role in the consolidation process. More recently, evidence has uncovered functional heterogeneity of pyramidal neurons within distinct sublayers of CA1 that display unique properties during ripples, potentially contributing to memory specificity. Despite this, it remains unclear exactly how ripples shift the activity of CA1 neuronal populations to accommodate the consolidation of specific memories and how sublayer differences manifest. Here, we studied interactions between the anterior cingulate cortex (ACC) and CA1 neurons during ripples and discovered a reorganization of their communication following learning. Specifically, using a generalized linear model decoder, we demonstrated the pre-existence of ACC-to-CA1 communication, which is weakened during post-training sleep following learning, suggesting that ACC activity reallocates the contribution of CA1 neurons during memory formation. Interestingly, the reorganization appeared unique for a subset of CA1 superficial (CA1sup) neurons that were task inactive, whereas communication between the ACC and CA1 deep neurons remained largely stable across pre- and post-training sleep. Consistent with this sublayer-selective reorganization, we found that optogenetic stimulations of the ACC preferentially suppressed CA1sup neurons while activating a unique subset of CA1 interneurons. Overall, these findings highlight an important role of the ACC in rebalancing CA1 neuronal populations' contribution in learning and memory consolidation.

Introduction

Memories are not static, rather they are gradually consolidated into long-term traces across days, weeks, or longer (Klinzing et al., 2019; Squire et al., 2015). At any given moment, we are processing and consolidating an array of differing experiences. The ability to preserve distinctiveness across these various experiences is essential for memory consolidation. This requires a delicate balance between the mechanisms that facilitate the reactivation and transformation of new memories alongside those which regulate consolidation to prevent the

intermingling of distinct experiences. While much attention has been focused on uncovering the principles that guide the reactivation and consolidation of memories, less is known about the mechanisms that regulate these processes and govern memory specificity.

During sleep, sharp-wave ripples, neural oscillations predominantly within the CA1 of the hippocampus, facilitate hippocampal reactivations and accompany cortical reactivations of memory-related neurons, a process referred to as replay (Buzsáki, 2015; Buzsáki et al., 1992; Davidson et al., 2009; Diba & Buzsáki, 2007; Foster & Wilson, 2006; Lee & Wilson, 2002). Replay has been shown to be essential for memory consolidation as disruption or enhancement of ripples impairs or improves memory, respectively (Ego-Stengel & Wilson, 2010; Fernández-Ruiz et al., 2019; Girardeau et al., 2009; Gridchyn et al., 2020; Jadhav et al., 2012; Wang et al., 2015). Recently, evidence has uncovered functional and anatomical heterogeneity in CA1 neurons based on their position within the pyramidal layer: the superficial (CA1sup) and deep (CA1deep) sublayers (Danielson et al., 2016; Geiller et al., 2017; Hall & Wang, 2023; Harvey et al., 2023; Mizuseki et al., 2011; Sharif et al., 2021). CA1sup neurons have more stable firing rates and higher spatial acuity (Danielson et al., 2016; Harvey et al., 2023; Mizuseki et al., 2011), whereas CA1deep neurons respond more to enriched environments, sensory landmarks, and reward (Danielson et al., 2016; Geiller et al., 2017; Harvey et al., 2023; Sharif et al., 2021). During replay events CA1sup neurons show increased activity after spatial learning, whereas CA1deep neurons show decreased activity (Berndt et al., 2023; Harvey et al., 2023). Together, ripples and the recruitment of distinct subpopulations within CA1 drive new memory formation. Despite this understanding, the mechanisms which regulate their activity to balance consolidation across experiences remain unclear.

Emerging evidence has demonstrated the importance of suppression within the hippocampal network to balance neuronal excitability surrounding learning (Gava et al., 2024; Karaba et al., 2024; Norimoto et al., 2018). During pre-learning sleep, ripples depotentiate synapses which, if perturbed, impairs learning (Norimoto et al., 2018). Similarly, after learning, ripples facilitate the depotentiation of memory-unrelated neurons (Norimoto et al., 2018). Additionally, during post-learning sleep, hippocampal neurons initially display heightened firing rates before ultimately returning to baseline (Giri et al., 2019; Wilson & McNaughton, 1994). Prior studies have demonstrated that reestablishing baseline is necessary for learning, as excessive neuronal activity and synchrony impairs learning (Gava et al., 2024; Karaba et al., 2024). Suppression of the hippocampus, then, appears to play a key role in down regulating synapses, preventing memory saturation, and promoting memory flexibility (Balduzzi & Tononi, 2013). Interestingly, CA1sup neurons appear to be the most sensitive to this process (Gava et al., 2024). Following repetitive learning, CA1sup neurons become highly synchronized and coactive, which impairs future memory formation (Gava et al., 2024). Correspondingly, optogenetic inhibition of CA1sup, but not CA1deep neurons, after learning decouples and decreases neuronal activity which reduces rigidity and restores new memory formation (Gava et al., 2024). Still, exactly how facilitation and suppression are balanced throughout consolidation, and whether cortical inputs play a role in modifying hippocampal activity in this process, remains poorly understood.

Here, we employ *in vivo* electrophysiology recording across contextual fear conditioning (CFC) and sleep to understand how communication between the anterior cingulate cortex (ACC) and hippocampal CA1 are modified following learning. Previous studies have shown that the ACC displays increased activity immediately preceding CA1 ripples and is instrumental in CFC and memory consolidation (Einarsson & Nader, 2012; Frankland et al., 2004; Wang & Ikemoto, 2016). We uncovered a novel, sublayer specific, line of communication between ACC and CA1 surrounding ripples with ACC preferentially communicating with CA1sup neurons. This communication rebalances following learning, suggesting a potential role in memory consolidation.

Results

Pre-ripple ACC activity predicts CA1 activity during ripples

To understand how the ACC and hippocampus communicate surrounding learning, we employed simultaneous dual-site *in vivo* electrophysiology recordings of both regions throughout a contextual fear conditioning paradigm (Figure 1A, B). In this approach, we were able to examine ACC–CA1 communication prior to, during, and after learning, enabling us to examine how this communication evolves across fear learning. Specifically, we emphasized investigation into communication changes between pre- and post-training sleep to understand whether functional connectivity undergoes learning-related reorganization. Local field potentials and neuronal spikes were recorded simultaneously, and slow-wave sleep was identified by CA1 delta-to-theta power ratio and the animal's immobility (Figure 1C) (Wang et al., 2015).

We first examined ACC neuronal spiking activity surrounding CA1 ripples during pre-training sleep. Across 10 mice, we recorded 303 ACC neurons, with individual counts per animal ranging between 19–48 neurons. Most ACC neurons (235/303) displayed significant changes in activity surrounding ripples compared to baseline (Figure 1D; see Methods). Of the neurons with significant changes, the majority displayed a pre-ripple activation (81.7%; 192/235) while a minority (18.3%; 43/235) showed a more prominent post-ripple activation (Figure 1D). To determine whether this coordinated activity is indicative of information flow, we implemented general linear model (GLM) machine learning decoding to test whether population ACC activity preceding ripples can predict CA1 activity during ripples (Figure 1E) (Jun Liu et al., 2024; Rothschild et al., 2017). ACC spiking was binned into 200 ms segments across multiple time windows to predict individual CA1 neuronal firing rates between 0–100 ms after ripple onset (Figure 1E; see Methods). The decoder was trained on 50% of the recorded data upon which the remaining 50% data was used for testing. All GLM decoding was performed on spike data recorded during slow-wave sleep epochs before or after training. We found that across multiple time-windows, prediction gain (PG) score using real data was significantly higher than shuffled (Figure 1F). PG score was greatest when using ACC spiking –200–0 ms preceding ripple onset, aligning with the observed correlated firing seen in Figure 1D. Moreover, only this window showed learning-related changes with a significant decrease in PG score in post-training sleep. In accordance, all subsequent GLM analyses in this paper will use the –200–0 ms time window (Figure 1F).

Our GLM analysis generated a PG score for each CA1 neuron, enabling us to examine how PG scores correlate and shift with other properties of CA1 neurons. We first asked whether the learning-related reduction in PG score reflected a global dampening of ACC→CA1 communication or a selective redistribution across CA1 neurons. To test this, we examined the stability of PG scores between pre- and post-training sleep. Preservation of PG score ranking among CA1 neurons would suggest that learning weakens existing ACC→CA1 communication while maintaining the relative contribution of individual ACC neurons, consistent with a global dampening effect. In contrast, poor preservation of PG score ranking would be more indicative of a reorganization of ACC→CA1 communication. We found that PG scores were positively correlated across sessions, that is, CA1 neurons with high PG scores before learning tended to retain relatively high PG score after learning (Figure 2A). To further assess the stability of PG score ranking, we performed permutation-based preservation analyses (Figure 2B). Neurons in the top PG score quartile were significantly more likely than expected by chance to remain in the top quartile following learning, whereas transitions between top and bottom quartiles were rare. Together, these findings suggest that functional connectivity between the ACC and CA1 is broadly dampened after learning rather than undergoing robust reorganization.

To examine ACC–CA1 communication independently of the GLM analysis, we computed spike-triggered averages (STA) of CA1 neuron activity using a pooled ACC spike train generated by merging spikes from all recorded ACC neurons. We performed a full lag-resolved analysis in which CA1 spike trains were aligned to ACC spike times, baseline-normalized, and quantified in 10-ms bins across a peri-ACC-spike window (Figure 1—figure supplement 1A, B). This analysis

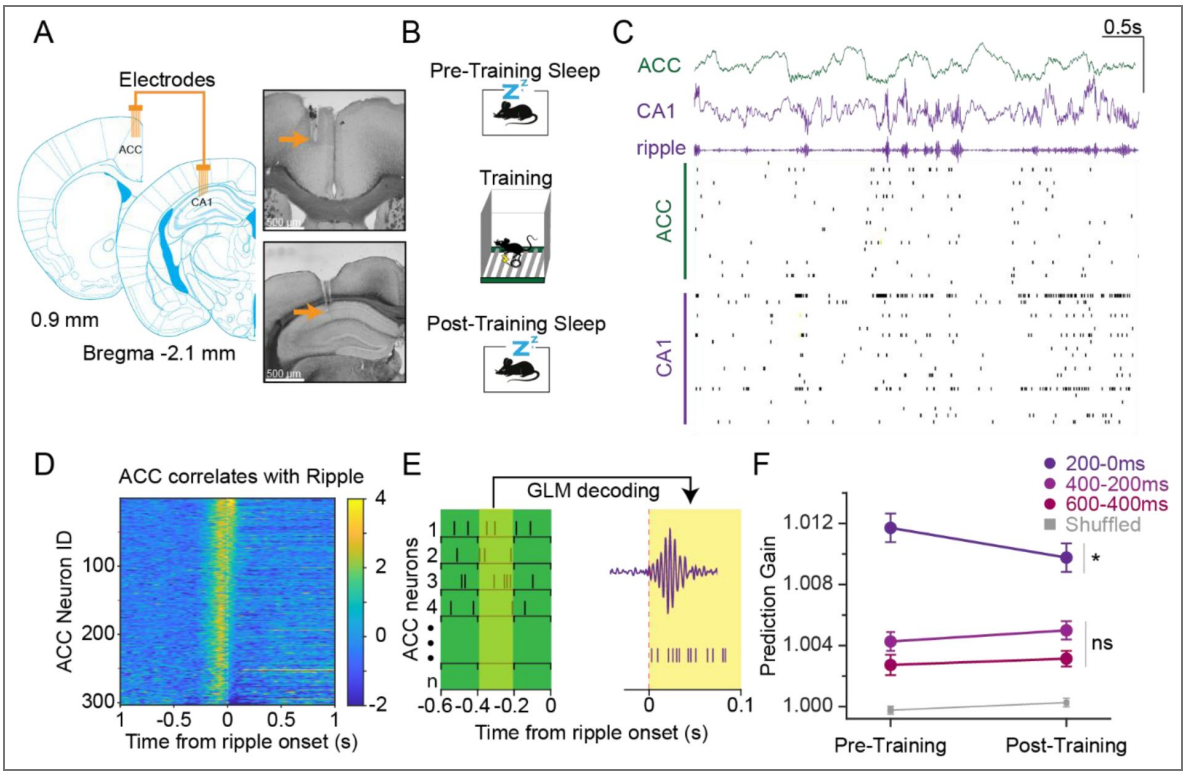

Figure 1. Pre-ripple ACC activity predicts CA1 activity during ripples

A, Left, schematic of a dual 8-tetrode array implanted in the ACC and CA1. Right, two representative brain sections highlighting the recording sites (orange arrows) in the ACC and CA1, top and bottom, respectively. **B**, Schematic of the contextual fear memory procedure. **C**, Top, Representative ACC and CA1 LFP from a pre-training sleep session, Y axis scale bar 1 mV. Bottom, individual spikes across ACC and CA1 neurons. **D**, Heatmap of ACC neuron (N = 10 animals; N = 303 neurons) activity during pre-training sleep surrounding ripple onsets (bin = 5 ms). **E**, Schematic of GLM decoder. 200 ms bins of ACC spiking data preceding ripple predict CA1 activity 0–100 ms after ripple onset. **F**, Prediction gain difference in decoding CA1 activity between real and shuffled ACC activity across three pre-ripple predictor windows (−200 to 0 ms, −400 to −200 ms, and −600 to −400 ms; N = 10 animals; N = 291 CA1 neurons). Repeated measures mixed-model analysis revealed a significant effect of predictor type, with real prediction gain exceeding shuffled prediction gain overall ($p < .001$), and a significant effect of predictor window ($p < .001$). There was also a significant effect of session (pre vs post) on prediction gain that varied across predictor windows (Window × session interaction, $p = .010$). Post-hoc comparisons showed that prediction gain was highest in the −200 to 0 ms window relative to earlier windows during pre- and post-training sleep (all Holm-corrected, $p < .001$). Additionally, the −200 to 0ms window exhibited a significant pre-to-post decrease in prediction gain (Wilcoxon signed-rank, $p = .022$), whereas the other windows did not. Error bars indicate ± SEM.

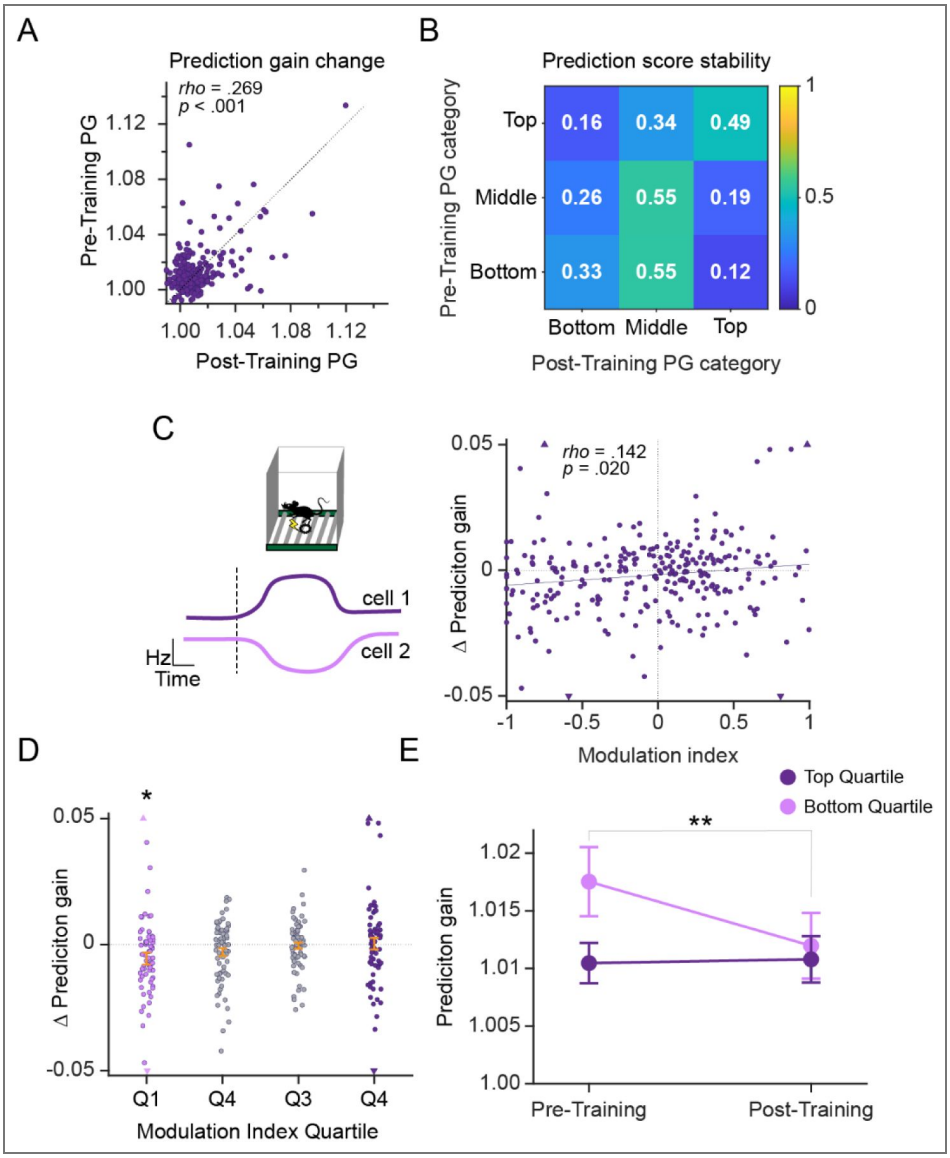

Figure 2. Learning dampens ACC→CA1 communication which differs based on task engagement.

A, Correlation of PG scores between pre- and post-training sleep (N = 10 animals; N = 291 CA1 neurons). Spearman's Rho revealed a significant correlation between pre- and post-training sleep, *rho* = .269 *p* < .001. **B**, PG score rank preservation permutation matrices. Permutation testing revealed that nearly half of CA1 neurons in the top PG score quartile remained in the top quartile after training (49.3%, permutation *p* < .001), significantly exceeding chance expectations. Whereas retention of bottom-quartile neurons was weaker, showing only a trend above chance (32.9%, permutation *p* = .052). Extreme transitions between top and bottom categories were uncommon and not enriched above chance (*p* = .999). **C**, Left, Schematic of two representative neurons' firing patterns during training, Neuron 1 increases and Neuron 2 decreases activity during training. Right, correlation scatter plot of CA1 neuron ΔPG and modulation index. Spearman's Rho revealed a modest positive correlation between variables, *rho* = .142, *p* = .020. Purple triangles indicate extreme values that were included in all statistical analyses but are cropped for visualization purposes. **D**, ΔPG as a function of modulation index quartiles (N = 66 per quartile). Overall quartile effect did not reach significance (Kruskal-Wallis, *p* = .081). **E**, PG scores as a function of task modulation. Neurons were divided into the top and bottom modulation index (MI) quartiles. A linear mixed-effects model revealed significant effects of MI quartile (*p* = .005) and session (*p* = .017), with a trend-level MI quartile × session interaction (*p* = .074). Post-hoc comparisons showed a significant pre-to-post reduction in PG score for neurons in the bottom MI quartile (Holm-corrected, *p* = .010), whereas neurons in the highest MI quartile showed no significant change (Holm-corrected, *p* = .831). Error bars indicate ± SEM.

revealed a significant reduction in CA1 activity following ACC population spiking in post-compared to pre-training sleep, suggesting a reduction in ACC–CA1 coupling after learning, consistent with the GLM decoding results.

Task-inactive CA1 neurons reshape their activity with ACC after learning

Since overall functional connectivity between ACC and CA1 changed after learning, we next asked whether PG scores across CA1 neurons differed based on their activity during training. To test this, we calculated a modulation index by comparing each CA1 neurons' firing rate during training with its pre-training baseline (Figure 2C) (Karaba et al., 2024). We found that predication gain change (ΔPG), showed a modest positive correlation with modulation index, indicating that task engagement modifies ACC→CA1 communication (Figure 2C). To investigate this relationship further, CA1 neurons were separated into modulation-index quartiles and their ΔPG were compared across quartiles. Although the overall effect of quartile did not reach significance in the linear mixed-effects model, neurons in the bottom quartile (task-inactive) exhibited a significant reduction in ΔPG, whereas no significant changes were observed in the remaining quartiles (Figure 2D). To better illustrate this effect, we next compared pre- and post-training PG scores in the top and bottom quartiles. Consistent with the ΔPG analysis, only neurons in the bottom quartile exhibited a significant reduction in PG scores following learning, suggesting that the that learning-related decreases in ACC→CA1 communication is primarily driven by a loss in functional connectivity with bottom quartile CA1 neurons (task-inactive) (Figure 2E). Lastly, we examined whether PG scores correlated with the freezing response in mice during recall. Across all mice, freezing was significantly higher during recall than pre-shock baseline during training (Figure 2—figure supplement 1A). Overall, we found no correlation between PG and freezing (Figure 2—figure supplement 1B–D). However, there was a trend for a positive correlation (p=.07) between ΔPG and freezing percentage. An important consideration is that the uniformly high levels of freezing in mice limited behavioral variability, potentially reducing our ability to detect relationships between ACC–CA1 communication decoding and behavioral differences.

ACC displays a distinct relationship with CA1 sublayers

It has been well established that functional heterogeneity exists within the pyramidal layer of CA1 (Hall & Wang, 2023; Mizuseki et al., 2011). To investigate whether ACC communication is different across CA1 sublayers, we separated CA1 neurons into CA1sup and CA1deep neurons based on their sharp-wave deflection characteristics (Figure 3A; for details see Methods) (Danielson et al., 2016; Mizuseki et al., 2011). We first asked whether CA1 sublayers displayed differences in GLM decoding after learning. Although PG score was significantly higher for each sublayer compared to shuffled, neither sublayer showed a learning-related difference (trend p = .058) nor was there a significant difference between sublayers (Figure 3B). While GLM decoding revealed similar PG scores across CA1 sublayers, it remains possible that the stability of predictive relationship differed between them. Therefore, we examined how well PG scores correlated between pre- and post-training sleep and the degree of retention for the highly predicted neurons. Our results show that CA1sup neurons showed no significant correlation in PG scores across sessions, and permutation testing revealed that the highly predicted neurons were not retained above chance levels (Figure 3C, D). In contrast, CA1deep neurons exhibited significant PG score preservation across sessions, with both positive pre-to-post correlations and above-chance retention for the highly predicted neurons (Figure 3E, F). Together, these results suggests that ACC→CA1sup communication is more dynamic and evolving across learning, whereas ACC→CA1deep communication remains comparatively stable.

Given the differences in PG score stability across CA1 sublayers, we next asked whether task engagement further influenced ACC→CA1 sublayer connectivity. We first examined whether ΔPG correlated with modulation index. In CA1sup neurons, we found a significant correlation between ΔPG and modulation index, suggesting that greater change in task engagement is associated with greater PG score change (Figure 4A). In support, ΔPG significantly differed across modulation

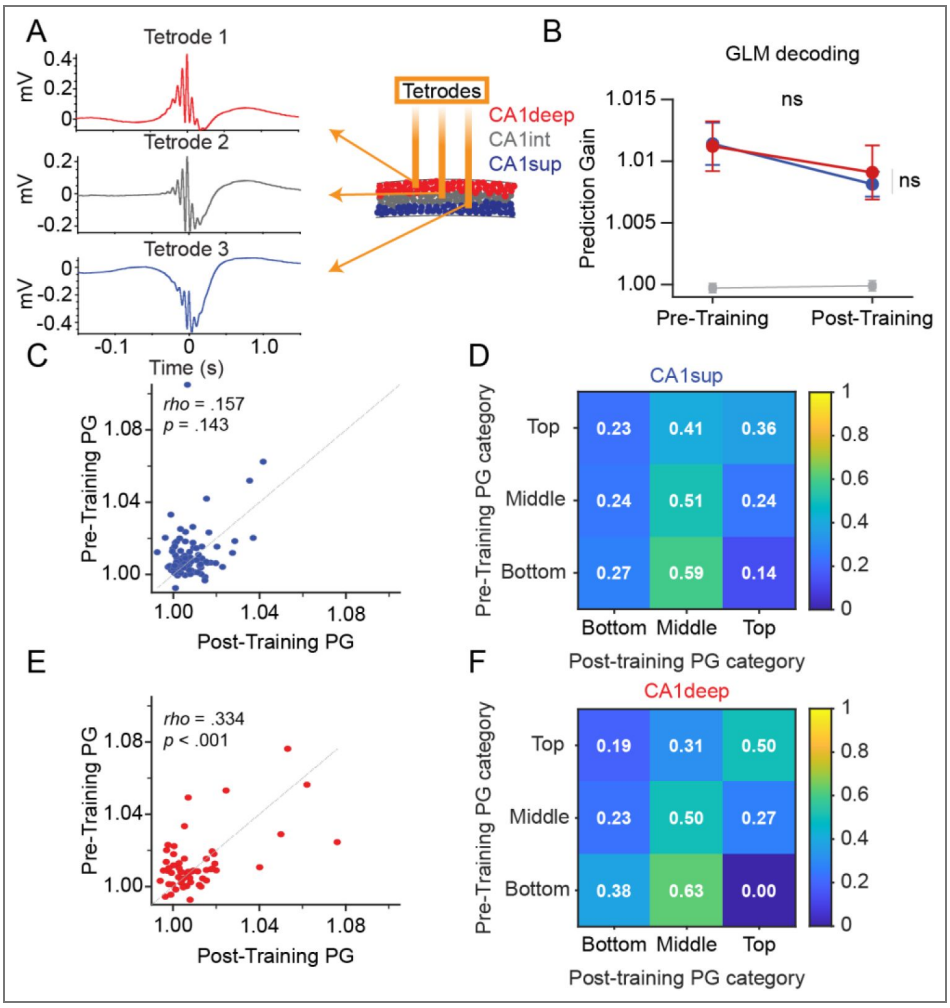

Figure 3. Prediction Gain stability differences between sublayers

A, Schematic of sublayer identification based on sharp-wave deflection difference across the pyramidal layer. **B,** PG scores before and after learning (N = 10 animals; CA1sup: N = 89; CA1deep: N = 61). Mixed-effects model revealed no significant difference in PG scores between sublayers (p = .755) but showed a trend for training session (p = .058*)*. **C**, Correlation scatter plot of PG score and modulation index for CA1sup neurons (N = 89). Spearman's Rho revealed no correlation between pre-training and post-training PG scores (*rho* = .157*; p* = .143). **D**, PG score rank preservation permutation matrices for CA1sup neurons (N = 89). Permutation testing revealed that neither top-quartile (36.4%, p = .121) nor bottom-quartile (27.3%, p = .484) retention exceeded chance levels. **E,** Correlation scatter plot of PG score and modulation index for CA1deep neurons (N = 61). Spearman's Rho revealed a significant positive correlation between pre- and post-training PG scores for CA1deep neurons (*rho* = *.334; p* < .001). **F**, PG score rank preservation permutation matrices for CA1deep neurons (N = 61). CA1deep neurons' top-quartile retention was 50.0% and significantly above chance, permutation p = .014. In contrast, bottom-quartile retention did not exceed chance levels, p = .174. Extreme top-to-bottom or bottom-to-top switching occurred in 8 CA1sup neurons (18.2%, p = .902) and 3 CA1 deep neurons (9.4% p = .998*)*. Error bars indicate ± SEM.

index quartiles for CA1sup neurons (Figure 4B). Interestingly, only bottom quartile neurons exhibited learning-dependent change in PG with a significant reduction after learning, suggesting that the reduction in ACC→CA1 communication is mediated primarily by the loss of connectivity with task-inactive CA1sup neurons (Figure 4B, C). Together, these results suggest that CA1sup neurons that are more strongly suppressed during new learning are more likely to become functionally decoupled with the ACC after learning. By contrast, CA1deep exhibited no significant changes across any of these measures further supporting more stable connectivity with ACC (Figure 4D–F). Finally, we examined ACC spike-triggered average of CA1 sublayers. CA1sup showed a significant pre-to-post reduction in baseline-subtracted STA response, whereas CA1deep did not (Figure 1—figure supplement 1). However, the direct comparison of pre-to-post change between CA1sup and CA1deep was not significant ($p = .09$).

Overall, ACC→CA1sup predictive relationships were less stable across pre- and post-training sleep, with learning-related reductions occurring specifically among task-inactive CA1 neurons. In contrast, ACC→CA1deep communication remained largely stable across learning. Together, these findings indicate that learning selectively remodels ACC communication with CA1sup neurons, whereas ACC→CA1deep communication is comparatively preserved.

Optogenetic stimulation of the ACC preferentially inhibits CA1sup neurons

To determine whether the ACC can directly influence the activity of CA1sup neurons, we performed optogenetic stimulation of ACC neurons in a separate cohort of mice while recording CA1 neurons during sleep. We microinjected AAV-CaMKII-ChR2 into the ACC and implanted an optic fiber above the injection site, alongside a recording tetrode array implanted into the CA1 ipsilaterally (Figure 5A—figure supplement 1). After allowing time for viral expression, we administered 4-pulse, 25-Hz optogenetic stimulations during sleep to examine how CA1 neurons responded to ACC stimulations. CA1sup neurons displayed prolonged activity changes, primarily suppression, whereas CA1deep showed limited responses (Figure 5C). To quantify CA1 sublayer differences, we normalized CA1 firing rates across the stimulation window (0–4 sec from stimulation onset) and compared pre-stim to post-stim normalized firing rate (Figure 5D). We found that CA1sup firing rate was significantly lower than CA1deep neurons during the 4 sec post-stim window. Of note, we replicated these stimulation parameters during wakefulness and found more muted responses across each sublayer, suggesting communication between ACC and CA1 is state-dependent (Figure 5—figure supplement 2). Overall, activating ACC produces long-lasting inhibition of CA1sup with limited impact over CA1deep neurons, supporting a selective ACC→CA1sup communication during sleep.

Optogenetic stimulation of the ACC differentially affects CA1 interneurons

Within CA1 lies a complex network of interneurons, which play critical roles in memory processes (Tzilivaki et al., 2023). We aimed to understand how local interneurons within CA1 respond to ACC stimulations. We first investigated the responses of fast-spiking putative parvalbumin (PV) interneurons. Their firing properties have been well characterized and have been shown to display increased activity during ripples (Figure 6 A–C; see Methods for details) (Klausberger & Somogyi, 2008; Opalka et al., 2020; Varga et al., 2014). Upon stimulation of the ACC during sleep, we discovered a robust inhibition of PV interneurons (Figure 6D, E). Like CA1sup neurons, PV suppression was delayed (median latency = 97.5 ms, IQR = 37.5–295 ms) and prolonged, demonstrating that the ACC can drive sustained suppression of both CA1sup and PV interneurons (Figure 5C; Figure 6E; Figure 6—figure supplement 1E).

Notably, CA1 LFPs exhibited a laser-evoked response peaking roughly 13 ms after ACC stimulation, which precedes many of the responses seen in PV interneurons and CA1sup neurons (median latency = 350 ms, IQR = 130–830 ms) (Figure 5B, C; Figure 6E; Figure 6—figure supplemental 1E). This suggests the presence of a different population of CA1 neurons that respond on a scale

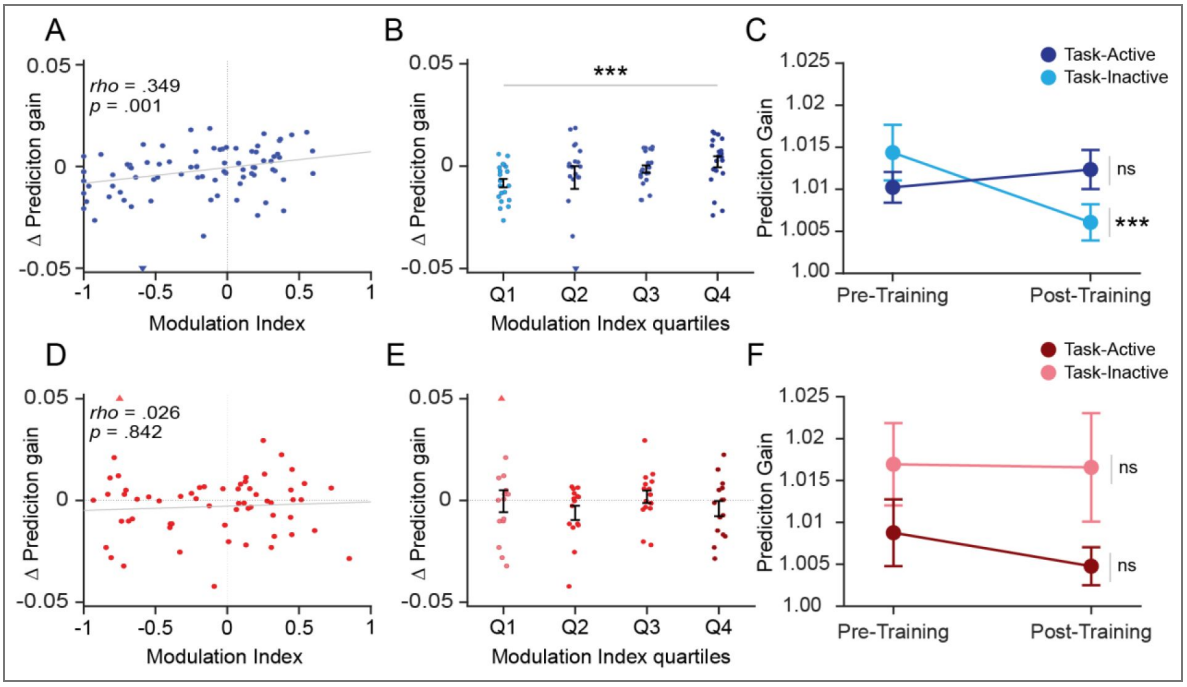

Figure 4. Sublayer differences in ACC→CA1 predictive communication as function of modulation index.

A–C, PG score differences across CA1sup neurons with respect to modulation index (N = 7 animals; CA1sup: N = 81). **A**, Correlation between CA1sup neurons' ΔPG and modulation index. Spearman's Rho revealed a significant positive correlation, *rho* = .349, $p < .001$). **B**, ΔPG as a function of modulation-index quartiles for CA1sup neurons (N = 81). A significant effect of modulation-index quartiles was observed (Kruskal-Wallis, $p = .014$). **C**, PG scores of top and bottom quartiles of CA1sup neurons. A linear mixed-effects model revealed a significant main effect of training session ($p < .001$) and quartile x session ($p = .002$). Post-hoc comparisons revealed a significant pre-to-post decrease in PG score for bottom quartile (Holm corrected, $p = .002$), with no change in top quartile neurons (Holm corrected, $p = .442$). **D–F,** PG score differences across CA1deep neurons with respect to modulation index (N = 6 animals; N = 61 CA1deep neurons). **D**, Correlation between neurons' PG score and modulation index. Spearman's Rho revealed a significant positive correlation between ΔPG and modulation index for CA1sup neurons, *rho* = .026, $p = .842$. **E**, ΔPG as a function of modulation-index quartiles for CA1deep neurons (N = 61). CA1deep exhibited no significant effect of modulation-index quartile was observed (Kruskal-Wallis, $p = .591$). **F,** PG scores of top and bottom quartiles of CA1 CA1deep neurons. A linear mixed-effects model did not reveal a significant main effect of training session ($p = .149$) or quartile x session interaction ($p = .934$). Likewise, post-hoc comparisons revealed no changes pre-to-post PG scores for either quartile (Bottom quartile: N = 15, Holm corrected, $p = .906$; Top quartile: N = 15, Holm corrected, $p = 1$). A linear mixed-effects model revealed a trend-level Modulation Index × Sublayer interaction ($p = .063$). Error bars indicate ± SEM.

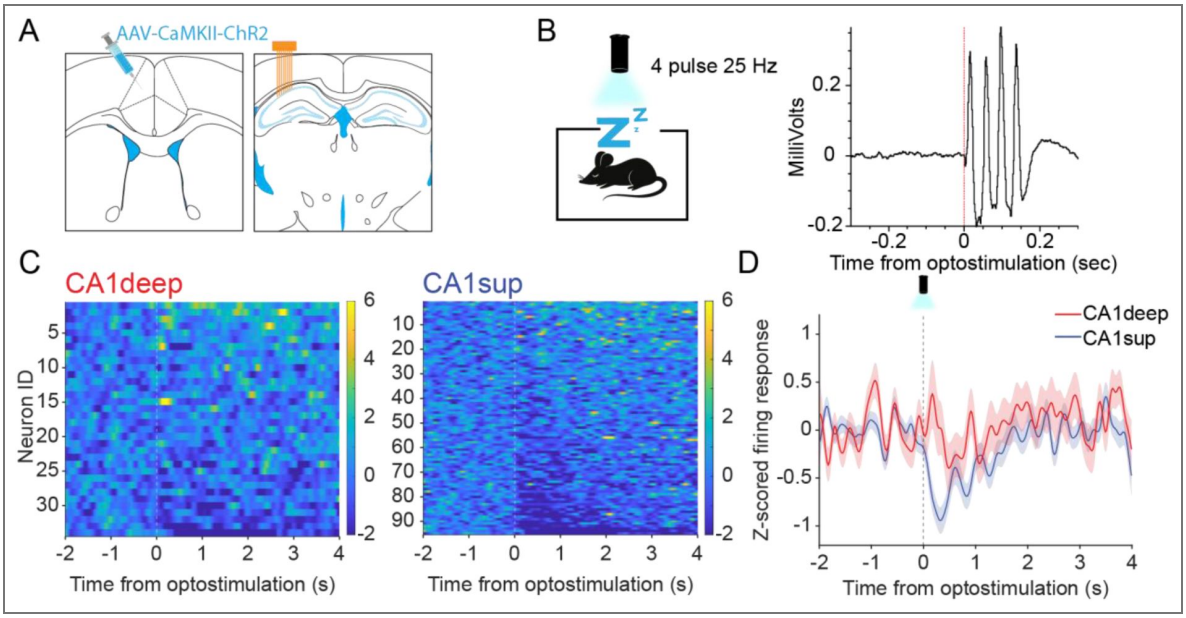

Figure 5. Optogenetic stimulation of the ACC preferentially inhibits CA1sup neurons.

A, Schematic of AAV injection and microdive implant. **B**, Left, schematic of optogenetic manipulation. Four pulse 25-Hz stimulations were performed during home-cage sleep. Right, representative CA1 LFP response to ACC stimulations. A fast peak, indicating maximal inhibition, occurs approximately 13 ms after stimulation onset. **C**, Heatmap activity CA1deep (N = 34) and CA1sup neurons (N = 96). **D**, Linear mixed-effects model revealed a significant Sublayer × Window interaction for the CA1 activity following ACC stimulation, $p = .022$. There was also an overall sublayer effect, $p = .037$. Post hoc between-sublayer comparisons showed that the strongest difference occurred in the 0–1 sec window, with CA1sup neurons showing greater suppression than CA1deep ($p < .01$, FDR-corrected, $q = .028$). Other time windows were not significantly different after FDR correction. Shaded region indicates mean ± SEM.

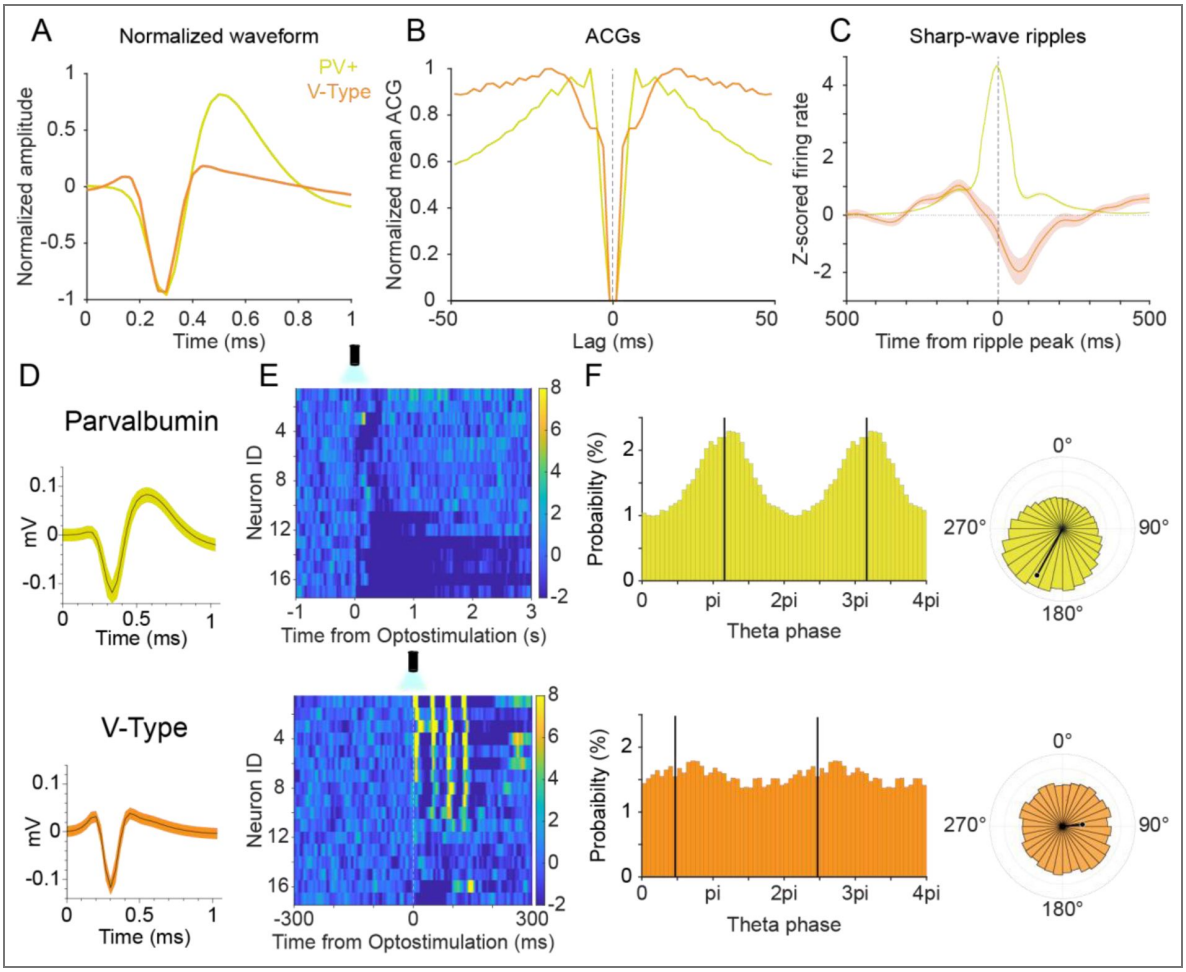

Figure 6. Optogenetic stimulation of the ACC differentially affects CA1 interneurons.

A, Normalized waveform of putative PV (N = 17) and V-type interneurons (N = 17). **B**, Autocorrelograms (ACGs) of putative PV and V-type interneurons across all spikes. ACGs were calculated for each putative PV and V-type interneuron, then averaged across all neurons within each group. **C**, Normalized firing across population PV and V-type interneurons during sharp-wave ripples. Mann-Whitney U revealed a significant difference in activity during sharp-wave ripples across interneurons, $p < .001$. **D**, Top, representative waveform of putative PV interneuron. Bottom, Representative waveform of a V-type interneuron. **E,** Top, Heatmap of PV interneurons spiking activity following stimulation of the ACC (bin size, 5 ms; N = 17). Bottom, Heatmap of V-type interneurons spiking activity following stimulation of the ACC (bin size, 1 ms; N = 17). **F**, Theta Phase-locking analysis and per-neuron circular statistics for CA1 interneurons during active wakefulness theta. Top, PV interneuron phase-locking response during theta. PV interneurons showed significant phase locking at 28.8° relative to trough, $r = -.795$, *Rayleigh* $p < .001$. Bottom, V-type interneuron phase-locking response during theta. V-type interneurons showed a per-neuron circular mean preferred phase of 84.5° relative to trough, however, this was not significant, $r = .385$, *Rayleigh* $p = .079$. Per-neuron circular statistics showed that PV and V-Type interneurons differed in preferred theta phase (Watson-Williams, $p < .001$) and phase-locking strength (Mann-Whitney U test, $p < .001$). Shaded region indicates mean ± SEM.

similar to that seen in the CA1 LFP. Throughout our recording sessions, we noticed a reoccurring neuron type that showed a V-shape spike waveform and distinct autocorrelegram (Figure 6A, B). Unlike PV interneurons and pyramidal neurons, these V-type interneurons decreased activity during ripples (Figure 6C). Most notable, however, was their robust, low-latency activation to ACC stimulations (median latency = 10.5 ms, IQR = 8.1–13.3 ms) (Figure 6D; Figure 6—figure supplement 1E). Overall, these V-type interneurons had a narrow spike width, were fast spiking (Hz), and displayed a distinct inter-spike interval pattern compared to PV interneurons and pyramidal cells (Figure 6—figure supplement 1). Unlike PV interneurons, V-type interneurons did not exhibit significant theta phase locking, instead firing more uniformly across the theta cycle, and displayed a significantly lower burst index (Figure 6F; Figure 6—figure supplement 1D). Given that V-type interneuron activation precedes suppression of pyramidal cells and PV interneurons after ACC stimulation, it is possible that V-type interneurons mediate the inhibition seen in pyramidal cells and PV interneurons. However, further studies are needed to identify and test whether these neurons influence CA1 network activity.

Discussion

Balancing network excitability with suppression after learning has long been thought to be essential for memory formation, with sleep serving a key homeostatic role (Liu et al., 2010; Tononi & Cirelli, 2003; Tononi & Cirelli, 2006; Watson et al., 2016) Excessive excitability and overly strengthened synapses can hinder neuronal flexibility and saturate the capacity for learning (Balduzzi & Tononi, 2013; Gava et al., 2024; Norimoto et al., 2018). Additionally, underregulated excitability may pathologically link multiple memory traces, leading to memory overgeneralization (Jinde et al., 2012; Kim et al., 2021). Therefore, regulatory mechanisms that rebalance the excitability of neurons to enable neuronal flexibility are essential for memory formation (Gava et al., 2024; Karaba et al., 2024). CA1sup neurons have been shown to be particularly susceptible to memory rigidity (Gava et al., 2024; Hall & Wang, 2023). While activation of these neurons is necessary for the encoding of new memories, their regulation and timely suppression appear equally important to evoke flexibility and enable *de novo* consolidation within the hippocampal network (Gava et al., 2024; Harvey et al., 2023). Our results reveal a rebalancing of communication between the ACC and CA1 following learning. This was most pronounced for CA1sup neurons as functional connectivity was dynamically reorganized between pre- and post-training sleep. In particular, pre-existing ACC-to-CA1sup communication was weakened for task-inactive neurons after learning. Furthermore, we found that optogenetic ACC stimulations preferentially inhibited CA1sup neurons. Overall, our study uncovers an ACC→CA1sup line of communication that adapts to learning, potentially playing a role in the rebalancing of network excitability for memory formation.

Learning selectively weakens ACC coupling with task-inactive CA1sup neurons

We implemented GLM machine learning to decode CA1 neuronal firing rates during ripples based off the spiking rates of large ACC neuronal populations preceding ripples (Rothschild et al., 2017). The underlying principles of this analysis posit that if ACC activity preceding ripples influences subsequent activity in CA1 during ripples, the specific activity pattern of ACC neurons (predictor cells) should hold relevancy over the outcome of CA1 neurons (predicted cells). We found this to be true across all sleep sessions and neuron types, with real ACC spiking data showing significantly higher prediction gain compared to shuffled data, indicating an information flow from ACC to CA1 surrounding ripples. Interestingly, prediction gain was weakened following learning specifically for task-inactive CA1sup neurons, suggesting a selective reorganization of communication with CA1sup neurons according to their recruitment during training. However, questions remain over exactly how the ACC influences CA1sup activity and why this information flow rebalances after learning.

One possible explanation is that ACC→CA1sup communication before training may reflect encoding of past experiences. Research has demonstrated that the ACC has a limited role in consolidation immediately after learning (Junyu Liu et al., 2024). Instead, memories become ACC-dependent beginning typically two days after learning (Einarsson & Nader, 2012; Frankland et al., 2004; Junyu Liu et al., 2024). It is possible that heightened pre-existing communication between ACC and CA1sup is reflective of consolidating past experiences. If true, decreased communication between regions may be due to the network's shift towards prioritizing the encoding/consolidating of the new experience and thus the role of the ACC to CA1, consolidating past memories, is reduced (Diekelmann & Born, 2010; Huelin Gorriz et al., 2023; Wilson & McNaughton, 1994). From a broader perspective, ACC→CA1 could function as part of default mode network activity, and learning induces network shift toward the newly acquired memory (Buckner et al., 2008; Raichle, 2015).

Alternatively, ACC→CA1 communication may contribute to the homeostatic downscaling of memory-unrelated synapses during sleep. Evidence finds that slow-wave sleep is strongly linked to downscaling of non-learning related neuron activity (Gulati et al., 2017; Liu et al., 2010; Tononi & Cirelli, 2003; Tononi & Cirelli, 2006; Watson et al., 2016). Slow-wave sleep ripples in particular depotentiate memory unrelated synapses (Gulati et al., 2017; Norimoto et al., 2018). In our study, we find that the learning-related reduction in communication between ACC and CA1 was selective for task-inactive neurons. Therefore, ACC→CA1sup communication may not simply weaken following learning but rather becomes selectively disengaged from task-inactive neurons, enabling homeostatic downscaling while preserving behaviorally relevant synapses (Liu et al., 2010; Norimoto et al., 2018; Tononi & Cirelli, 2003; Tononi & Cirelli, 2006; Watson et al., 2016). Interestingly, behavioral recruitment alone cannot account for the observed remodeling of ACC→CA1 communication, as CA1sup and CA1deep neurons did not display significant differences in task-related activity (Figure 2—figure supplemental 2). Instead, these learning related changes of task inactive neurons appear sublayer specific.

A potential mechanism supporting this selectivity is suggested by our optogenetic findings, which revealed preferential suppression of CA1sup neurons following ACC stimulations. ACC-mediated inhibition may contribute to the gradual disengagement of subsets of CA1sup neurons overtime as memories transition toward long-term storage (Karaba et al., 2024; Raven & Aton, 2021). Such a mechanism would align with ACC's known role in systems consolidation and be particularly useful in the regulation of CA1sup neurons as they have been shown to be susceptible to memory rigidity and overgeneralization (Einarsson & Nader, 2012; Frankland et al., 2004; Gava et al., 2024; Junyu Liu et al., 2024). Future experiments casually manipulating this communication are needed to determine whether ACC activity directly influences the downregulation of CA1sup activity during training, or whether these regions are correlated partners whose activity is ultimately mediated by an external brain region.

As research investigating CA1 heterogeneity continues to gain attention, functional distinctions across different behaviors have emerged (Hall & Wang, 2023). Previous research has found that CA1deep neurons are more involved in reward and sensory landmark encoding, while CA1sup neurons are more involved in context and spatial encoding (Danielson et al., 2016; Geiller et al., 2017; Harvey et al., 2023). Moreover, CA1deep place cells are more likely to remap in response to local cue changes than CA1sup place cells (Esparza et al., 2025). There have been conflicting reports over which sublayer is more involved in learning and replay and which neurons are more plastic or rigid in response to learning (Berndt et al., 2023; Geiller et al., 2017; Grosmark & Buzsáki, 2016; Hall & Wang, 2023; Harvey et al., 2023). We speculate that it may depend on the behavioral task and the relevant upstream circuits that differentially recruit CA1 sublayers (Masurkar et al., 2017). Past reports, which have shown that CA1sup neurons are more involved in memory replay, implemented spatial learning tasks (Berndt et al., 2023; Harvey et al., 2023). In contrast, CA1deep neurons have been shown to be more important for encoding non-spatial aspects of memories, such as reward (Danielson et al., 2016; Harvey et al., 2023). In our study, we did not observe clear differences in sublayer responses to contextual fear conditioning. Instead, we uncovered a pathway specific difference with

ACC→CA1sup displaying a more plastic-like phenotype in response to learning compared to ACC→CA1deep. These findings, along with past reports, suggest that functional differences between CA1 sublayers may be better understood in the context of the specific behavioral and upstream circuits engaged during learning rather than as fixed “plastic” or “rigid” properties of the sublayers themselves (Masurkar et al., 2017). In fact, recent findings further complicate this notion, demonstrating sublayer differences emerging between two classes of ripples that differ based on current source density profiles (Castelli et al., 2025). Ultimately, future studies are needed to fully dissect the functional differences among CA1 sublayers and their inputs during ripples and across behaviors.

Lastly, our CA1 sublayer classification does come with its own caveats. Tetrode identification of CA1 sublayers is not a trivial matter. We implemented guidelines informed by past research (see Methods) to help ensure we isolated CA1sup and CA1deep groups, only including neurons where we had the greatest confidence (Berndt et al., 2023; Mizuseki et al., 2011). In doing so, we excluded neurons which classification was uncertain. It is possible this excludes some meaningful populations of CA1 sublayers. Additionally, despite our approach, some cross-inclusion of sublayers may remain. Therefore, interpretations of CA1 sublayers difference should be considered with these limitations in mind. That said, the number of neurons and animals tested does provide overall confidence regarding our results. Future studies investigating this ACC to CA1 sublayer specific line of communication would benefit from the use of silicon probes or neuropixels that enable precise radial localization. Another caveat to mention is that both the ACC and CA1 are involved in the stress response (Kim et al., 2015; Lamotte et al., 2021). Future experiments utilizing appetitive learning paradigms, rather than the aversive contextual fear conditioning used here, will help disentangle learning-related remodeling of ACC→CA1 communication from changes driven by stress.

Optogenetic stimulation of the ACC inhibits CA1sup neurons and PV interneurons

We found that direct stimulation of ACC excitatory neurons inhibited CA1sup and PV interneurons. Notably, these responses were delayed for CA1sup and PV interneurons, indicating polysynaptic connectivity (Piñol et al., 2012). Additionally, both neuron types exhibited sustained suppression in response to stimulations suggesting that the ACC may have an indirect and broad influence over CA1 network activity rather than a direct and transient role. Sustained inhibition over certain populations of pyramidal neurons and PV interneurons may support a rebalancing of network excitability, especially during sleep (Diekelmann & Born, 2010; Norimoto et al., 2018; Tononi & Cirelli, 2003).

The identification of V-type neurons may help explain responses seen in CA1sup and PV interneurons. These neurons displayed the lowest latency responses to stimulations and produced brief excitatory bursts indicative of an initial response to ACC stimulations (Piñol et al., 2012). These interneurons decreased their activity during ripples, a pattern that overlaps with *Sncg*-expressing CCK basket cells and inhibitor of DNA binding 2 (ID2) neurons (Dudok et al., 2021; Karaba et al., 2024; Valero et al., 2025; Vancura et al., 2023). It is possible that V-type neurons may overlap with these interneurons. Correspondence with CCK cell activity is of particular interest, given the role of CCK interneurons in CA1 circuitry. Namely, CCK interneurons are known to target CA1sup and PV interneurons and induce long-term excitability changes as seen in our optogenetic experiments (Hefft & Jonas, 2005; Karson et al., 2009; Klausberger et al., 2005; Valero et al., 2015). More recently, CCK interneurons have been identified as playing a causal role in regulating the excitability of CA1 neurons during ripples (Karaba et al., 2024). Together, this suggests a possible ACC influence on CA1 CCK interneurons, which provides sustained inhibition of CA1 pyramidal and PV interneurons during sleep in facilitating memory formation. One discrepancy, however, is that both CCK and ID2 neurons exhibit theta phase preference, which we found no evidence for in V-type interneuron (Klausberger et al., 2005; Valero et al.,

2025). Ultimately, our interpretations of V-type identity remain speculative as further studies are needed to characterize their activity, and casual experiments are required to completely elucidate their role.

Another important caveat to mention is that it remains an ongoing debate whether ACC directly projects to CA1 (Andrianova et al., 2023; Rajasethupathy et al., 2015; Shi et al., 2022). One lab reported monosynaptic ACC to CA1 connection (Rajasethupathy et al., 2015), while another lab replicated those same experiments but were unable to come to the same conclusions (Andrianova et al., 2023). Further studies report no direct connection (Shi et al., 2022). The contention in connectivity may arise from differences in targeting strategies, injection coordinates, or viruses used. Our findings reported an excitatory response in CA1 V-type interneurons in response to ACC stimulations, proposing another possibility for ACC→CA1 connectivity. Interestingly, V-type interneurons responded with low-latency as fast as 4.2 ms after stimulations, compatible with monosynaptic timing (Cho et al., 2013; Petreanu et al., 2007; Wang et al., 2009). If the ACC→V-Type connection was a monosynaptic pathway, it could help explain discrepancies in the field, as the relative sparsity of V-type interneurons may reduce the likelihood of detecting ACC→CA1 connectivity. However, future anatomical studies are needed to conclusively determine connectivity.

Alternatively, ACC→CA1 communication may be mediated by multiple intermediate structures (Behzadi et al., 1990; Oh et al., 2014; Shi et al., 2022; Souza et al., 2022). The ACC sends monosynaptic projections to the nucleus reuniens (RE) and median raphe (MnR), both of which project directly to CA1 (Oh et al., 2014; Shi et al., 2022). The RE has a known role in contextual discrimination learning and memory specificity (Ramanathan & Maren, 2019; Ramanathan et al., 2018; Ratigan et al., 2023; Silva et al., 2021; Xu & Südhof, 2013). Interestingly, RE→CA1 activity tuned to immobility (freezing) emerges only after shocks are presented, suggesting a learning induced modification between regions, similar to that seen in our ACC–CA1 data (Ratigan et al., 2023). As for MnR, it receives dense inputs from the ACC (Behzadi et al., 1990; Souza et al., 2022), and its projections to the CA1 are predominantly glutamatergic (Jackson et al., 2009; Senft et al., 2021; Szonyi et al., 2016). Notably, these glutamatergic MnR inputs directly target CA1 interneurons, including CCK basket cells (Miettinen & Freund, 1992; Morales & Bloom, 1997; Senft et al., 2021), while avoiding PV interneurons and pyramidal neurons (Acsady et al., 1993; Freund et al., 1990; Halasy et al., 1992; Miettinen & Freund, 1992; Papp et al., 1999; Turi et al., 2019). This connectivity suggests that the ACC may indirectly modulate CA1 activity through the MnR, potentially suppressing PV interneuron and pyramidal neuron activity via local inhibitory circuits, thereby contributing to the regulation of hippocampal oscillations and memory consolidation (Huang et al., 2022; Wang et al., 2015). Ultimately, future experiments combining pathway-specific manipulations with simultaneous recordings will be necessary to distinguish direct from polysynaptic mechanisms.

Methods

Mice

Male C57BL/6 mice were purchased from the Jackson Laboratory (stock #000664). Mice were 3–4 months old at the time of surgery; after surgery, they were singly housed in cages (40 × 20 × 25 cm) containing corn cob and cotton material and kept on a 12 h light/dark cycle with *ad libitum* access to food and water. Experimental procedures were approved by the Institutional Animal Care and Use Committees of Drexel University (protocol # LA-23-740) and were in accordance with the National Research Council *Guide for the Care and Use of Laboratory Animals*.

Stereotaxic surgery

Surgery procedures were similar to that used in our lab (Huang et al., 2026; Jun Liu et al., 2024; Liu et al., 2021). In brief, mice were anesthetized with ketamine/xylazine mixture (~100/10 mg/kg, i.p.) and kept on a heating pad at 37°C. For *in vivo* electrophysiology recording, mice received implantation of two electrode arrays (8 tetrodes each) into the ACC and CA1,

respectively (Lin et al., 2006). For optogenetic stimulation, mice received intra-ACC microinjection of AAV viruses (AAV1-CKIIa-ChR2-GFP; 0.250 µl; ~10^{13} GC/ml; *Addgene* 105669) and implantation of one optic fiber (diameter 200 µm) slightly above the injection site; meanwhile, they received implantation of 8 tetrodes into the CA1 unilaterally on the ipsilateral side. AAV vectors were microinjected through a syringe pump (*World Precision Instruments*) over 5 min (50 nL/min), with an additional 5 min waiting period before removal of the injection needle (34 gauge, beveled). ACC coordinates from Bregma were AP 0.9 mm, ML 0.3 mm, DV 1.0 mm; CA1 coordinates from Bregma were AP –2.1 mm, ML 1.7 mm, and DV 1.1 mm.

In vivo electrophysiology

Each tetrode consisted of four wires (90% platinum 10% iridium; 18 µm diameter; *California Fine Wire*). A microdrive was used to couple with the electrode array, similar to that used in our lab (Jun Liu et al., 2024; Liu et al., 2021; Wang et al., 2015). Neural signal was preamplified, digitized, and recorded using a *Blackrock Neurotech* CerePlex. The local field potentials (LFPs) were digitized at 2 kHz and filtered at 500 Hz low cut; spikes were digitized at 30 kHz and filtered between 600–6000 Hz. The tetrode arrays were gradually lowered daily until we recorded clear ripples and a substantial number of neurons; otherwise, mice were excluded from the study. The recorded spikes were sorted manually using *Plexon* Offline Sorter. For dual-site experiments, spikes from 10 mice were used for analyses in this study; the neuron numbers in ACC and CA1 were 48/27, 35/50, 28/12, 32/27*, 22/29, 26/17, 28/33,19/17, 27/47, and 38/32 respectively. For optogenetic and *in* vivo electrophysiology experiments, 5 mice were used. The neurons numbers in CA1 were: 35, 30, 10, 38, and 24.

* This animal is missing the recording file during training and therefore was excluded from analyses comparing task active/inactive and firing rate ratios during training.

Optogenetics manipulations

Following surgery, mice were given 1 week for recovery and viral expression development. During recording, mice received 4-pulse 25-Hz stimulations (20-sec inter-trial interval). Laser stimulations ranged between 5–8 mW (473 nm wavelength). Laser intensity was tuned for each recording session until stimulation evoked a >0.2 mV change in CA1 LFP.

Ripples

Local field potentials were band-pass filtered between 100–250 Hz and ripple envelope was smoothed with a Gaussian kernel (S.D. = 4 ms) (Karlsson & Frank, 2009). We defined ripple amplitudes as the peak values of ripple envelopes. Only ripples with amplitudes exceeding 5 s.d. above the mean were used for analyses. For each ripple, onset and offset were taken as the earliest and latest time points where the ripple amplitude exceeded 1 SD above the mean around the ripple peak. Ripple duration was the difference between ripple onset and offset. Ripples less than 20 ms were excluded from the analysis.

Modulation and Burst index

Modulation index was a firing rate ratio calculated by comparing spiking during training with pre-training sleep baseline) (Girardeau et al., 2017; Karaba et al., 2024; Oliva et al., 2020). Equation: Modulation index = (Train – Pretrain) / (Train + Pretrain), in which Train and Pretrain are the average spikes per second for each CA1 neuron calculated during training and pre-training sleep, respectively. Burst index was defined as the fraction of consecutive inter-spike intervals shorter than 6 ms across the full session recording (Harris et al., 2001).

GLM decoding

We constructed generalized linear models (GLMs) with a log link function to predict spike counts of individual CA1 neurons during ripples based on population spike counts in ACC across specific time windows (Jun Liu et al., 2024; Rothschild et al., 2017). Spike counts of each ACC neuron were binned in 200-ms bins relative to ripple onset: −600 to −400 ms, −400 to −200 ms, −200 to 0 ms

to predict CA1 activity 0–100 ms. We randomly partitioned the ripples into two approximately two equally sized datasets: one of them was used to train the GLM decoder, and the other was used for testing. The model derived from the training phase was applied to the ACC population spike data in the test set, yielding predictions for the predicted CA1 spike counts across ripples. We calculated a prediction error for each CA1 neuron that was the mean absolute error between the predicted spike rate and real spike rate. We replicated this same analysis for shuffled data; wherein shuffled error distribution was generated by randomly permuting the predicted CA1 spike counts across ripple events. Prediction gain scores were derived by dividing shuffled prediction error by the real prediction error. Slow-wave sleep was determined by animals' immobility and the theta (6–12 Hz) /delta (1–4 Hz) ratio extracted from the local field potentials. A ratio of 1 or lower was identified as SWS, only epochs greater than 10 min were selected (Wang et al., 2015).

ACC activity surrounding ripples

To calculate significant differences in ACC activity surrounding ripples, we computed peri-ripple event histograms (smoothed with a three-bin Gaussian filter; bin size, 5 ms) for individual ACC neurons. We then compared ACC spiking activity between two 250 ms windows starting either –200 ms or –2000 ms (baseline) before ripple onset. 235 neurons (94%) showed significant increase from baseline (Wilcoxon-signed rank $p < .01$). Pre- or post-ripple peaks were determined whether a neurons firing rate peaked before (–200 to 0 ms) or after (0–200 ms) ripple onset.

Classification of CA1 pyramidal and interneurons

Putative excitatory (pyramidal) neurons and parvalbumin fast-spiking interneurons were classified based on spike waveform, firing rate, and spike width (Opalka et al., 2020) (Figure 6—figure supplement 1A–C). V-type interneurons were classified based on waveform, firing rate, spike width, and decreased ripple-correlated activity (Figure 6—figure supplement 1A–C). For sublayer classification, we examined the mean amplitude of the sharp wave deflection at maximum ripple power for each tetrode. Sharp-wave deflections that were greater than 50 μV were classified as CA1deep sublayer, whereas deflections less than –50 μV were classified as CA1sup sublayer. Any deflections between –50 and 50 μV were treated as intermediate and were excluded from sublayer analyses (Figure 3A).

Response latency to ACC optogenetic stimulations

Neural activity following stimulation onset was binned (CA1sup, 20 ms; PV, 5 ms; V-type, 0.1 ms) and z scored. For PV interneurons and CA1sup neurons, response latency was obtained by selecting the first bin where a neuron showed a difference from the baseline by a z-score of ± 2 or more (minimum for 3 consecutive bins). Because V-type interneurons exhibited substantially shorter response latencies, a higher temporal resolution analysis was performed. Spikes were aligned to four-pulse optogenetic stimulation trains and binned at 0.1-ms resolution. Firing rates during inter-pulse windows were z-scored relative to baseline, and response latency was defined as the time from stimulation onset to the peak response in the window with the strongest activation. Only neurons with a maximal response of $z \geq 5$ were included in the latency analysis.

Spike-theta phase locking

Theta oscillations were obtained from CA1 LFPs filtered at 6–12 Hz using a zero-phase filter in MATLAB (bandpass IIR filter; filter order = 8). Theta phase was estimated by Hilbert transformation of the filtered signal. For each neuron, spike times occurring during selected theta epochs were matched to the nearest LFP sample, and the corresponding instantaneous theta phase was extracted for circular statistical analysis. Phase locking was quantified using CircStat functions (Berens, 2009). We used standard Rayleigh test to determine uniformity of phase distribution (Totah et al., 2013), in which the p value for circular uniformity is calculated as follows:

$$p = \exp\left(sqrt\left(1 + 4 * n + 4 * \left(n^2 - R^2\right)\right) - (1 + 2 * n)\right)$$

and Rayleigh's z to determine the strength of spike–LFP phase locking as follows:

$$z = R^2/n$$

where *R* is the sum of resultant vectors across *n* spikes. Log-transformed Rayleigh z values were calculated log z values and stored for each neuron/group.

Spike Triggered Average (STA)

For each CA1 neuron, all ACC spikes recorded during slow-wave sleep in that same session were pooled and used as reference events. The spike times of each CA1 neuron were aligned to the pooled ACC spike. Relative CA1 spike times were counted in 10-ms bins over a window spanning −200 to 300 ms relative to the pool ACC spike. Spike counts within each lag bin were summed across all ACC spikes and converted to firing rate (Hz) by dividing by the total number of ACC spikes and the bin width. To normalize each neuron's lag-resolved STA, the mean firing rate during the −200 to −100 ms pre-ACC-spike baseline window was subtracted from every lag bin for that neuron. Thus, the normalized STA curve estimates the change in CA1 firing rate relative to the pre-ACC-spike baseline as a function of time from ACC spiking. Full-lag significance was assessed using an animal-level sign-flip cluster permutation test (Maris & Oostenveld, 2007). Post-minus-Pre STA difference curves were calculated for each animal, contiguous lag bins exceeding an uncorrected paired-test threshold were grouped into clusters and observed cluster masses were compared against a 5000-permutation sign-flip null distribution.

Fear conditioning (*in vivo* recording)

The fear-conditioning chamber used in the experiment was a square chamber measuring 25 × 25 × 32 cm, with a 36-bar shock grid floor (*Med Associates*). The behaviors of the mice were recorded using *Blackrock Neurotech NeuroMotive* video system. During training, the mice were first allowed to explore the footshock chamber for 3 minutes. They then received 3 mild footshocks (0.75 mA, 0.5 sec), with a 2-min interval between shocks. About 30 seconds after the last shock, the mice were returned to their home cages. After ~2 hours of post-training sleep, the mice were placed back in the footshock chamber for a 5-min contextual fear test. Neural activity was recorded continuously, including the pre-training sleep (2–3 hours), training (7.5 min), post-training sleep (2–3 hours), and contextual-fear test (5 min). Freezing was defined as the absence of visible movement expect for respiration as previously described and was scored continuously during the recall test (Anagnostaras et al., 2003; DeLorey et al., 1998). Percent Freezing was defined as time spent freezing divided by total time in recall (or pre-shock baseline during CFC). Additionally, the day prior to fear conditioning, mice were placed into a novel box for 7.5 min; neural activity was recorded across the pre-exposure sleep, exposure, and post-exposure sleep phases, to act as a behavioral control, however, these datasets were not analyzed for this manuscript.

Histology

To mark the final recording sites, we made electrical lesions by passing 20-second, 10-μA currents through two or more tetrodes. Mice were deeply anesthetized and intracardially perfused with ice-cold PBS or saline, followed by 10% formalin. The brains were removed and postfixed in formalin for at least 24 hours. The brains were sliced into coronal sections of 50-μm thickness using *Leica* vibratome. Sections were mounted with Mowiol mounting medium mixed with DAPI for microscopic examination of electrode placements, viral vector expression, and/or optical fiber placements.

Statistics

Sample sizes were based on previous similar studies in our labs (Jun Liu et al., 2024; Liu et al., 2021; Wang et al., 2015). Other statistical analyses include Freidman's test, Wilcoxon signed-rank test, Mann-Whitney U test, Kruskal-Wallis test, Welch's t-test, independent sample's t-test, and Student's *t* test. All statistical tests were two-sided. P-values of 0.05 or lower were considered significant. Non-parametric tests were utilized when normality assumptions failed.

Supplementary Figures

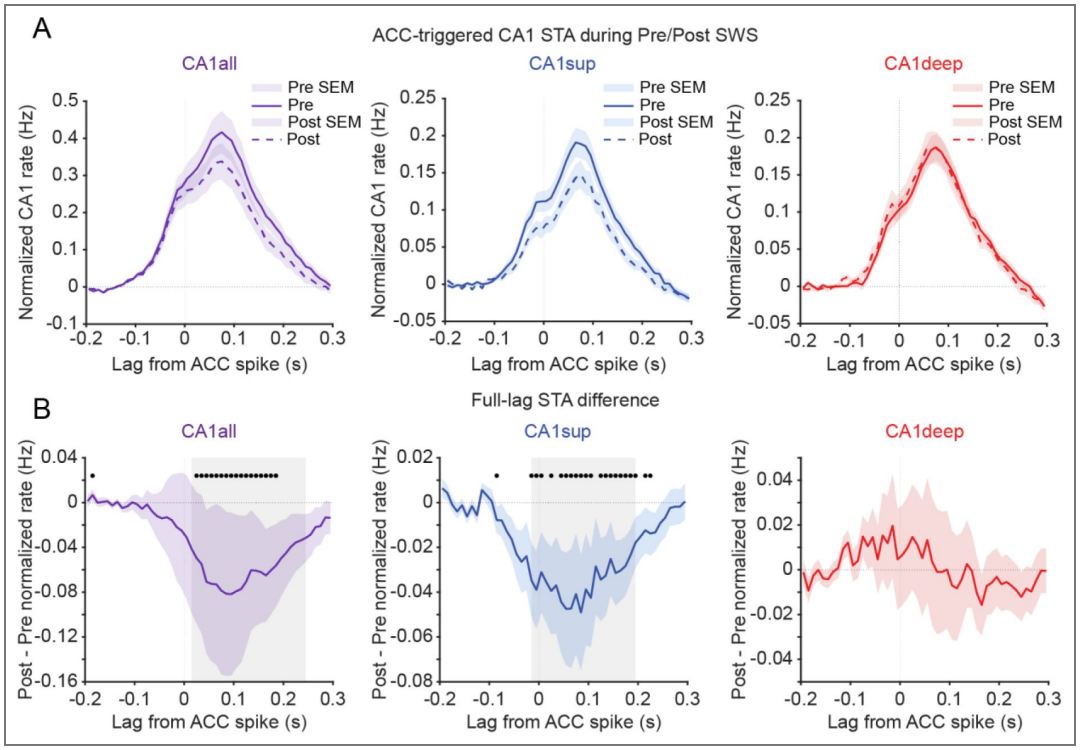

Figure 1—figure supplement 1. ACC→CA1 coupling decreases for CA1sup neurons, A, ACC-triggered CA1 spike-triggered averages during pre- and post-training SWS, normalized to each neuron's −200 to −100 ms pre-ACC-spike baseline for all CA1 neurons (left; N = 291), CA1sup (middle; N = 89) and CA1deep (right; N = 62). **B**, post-training minus pre-training STA difference curves. Black dots indicate lag bins surviving Benjamini–Hochberg false discovery rate (FDR) correction, and gray shading denotes significant clusters identified by an animal-level sign-flip cluster permutation test. Left, CA1 neurons exhibited a significant negative cluster spanning 15–245 ms after ACC spikes (cluster permutation, $p = .003$). Middle, CA1sup neurons similarly exhibited a significant negative cluster spanning −15 to 195 ms relative to ACC spikes (cluster permutation, $p = .008$). Right, no significant cluster was detected in CA1deep neurons (cluster permutation, $p = .240$). Consistent with the full-lag analysis, animal-level baseline-subtracted STA responses were significantly reduced following learning in CA1 neurons (N = 10, paired *t*-test, $p = .008$) and CA1sup neurons (N = 8, paired *t*-test, $p = .015$), but not in CA1deep neurons (N = 7, paired *t*-test, $p = .838$). Direct comparison of animal-level pre-to-post STA changes between CA1sup and CA1deep was not significant (Mann–Whitney *U* test, $p = .093$). Data not shown.

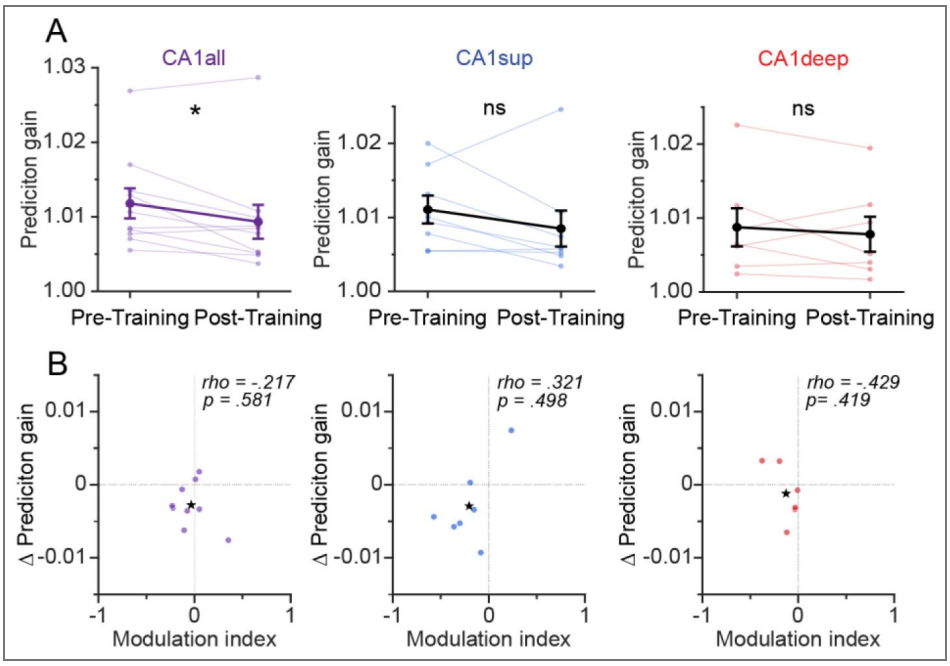

Figure 1—figure supplement 2. Prediction gain differences per animal,

A, Prediction gain differences between CA1 neurons across neurons grouped by animal. Left, Prediction gain difference across all recorded CA1 neurons averaged across animals (N = 10) across pre- and post-training sleep. Wilcoxon signed-ranked test revealed a significant pre-to-post decrease in prediction gain across animal, p = .048. Middle, prediction gain averaged across all recorded CA1sup neurons per animal (N = 8) across pre- and post-training sleep. Wilcoxon signed-ranked test found no significant differences pre to post decrease in prediction gain across animal, p = .250. Right, prediction gain difference across all recorded CA1deep neurons averaged per animal (N = 7) across pre- and post-training sleep. Wilcoxon signed-ranked test found no significant differences in prediction gain for CA1deep neurons across training sessions averaged across animal, p = .575. **B,** Correlations between modulation index and ΔPG for all CA1 neurons (N = 9), CA1sup (N = 7), and CA1deep (N = 6) per animal. Left, there was no significant correlation between modulation index ΔPG on a per animal basis for all CA1 neurons (Spearman's *rho* = -.217, p = .581. Middle, there was no significant correlation between modulation index ΔPG on a per animal basis for CA1sup neurons (Spearman's *rho* = .321, p = .498. Right, Likewise, there was no significant correlation between modulation index ΔPG on a per animal basis for CA1deep neurons (Spearman's *rho* = -.429, p = .419). Error bars indicate SEM.

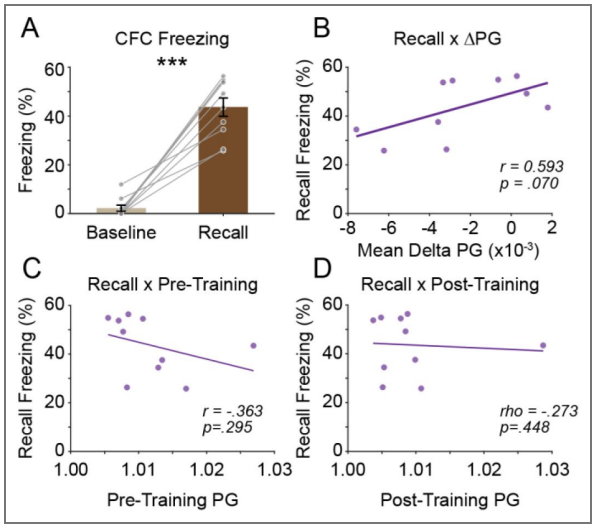

Figure 2—figure supplement 1. CFC freezing response correlated with Prediction gain,

A, Time spent freezing during CFC baseline and recall. Paired t-test revealed a significant difference in time spent freezing between BL and recall, $p < .001$ *(*N = 10 animals). **B**, Correlational analysis between time spent freezing during recall and prediction gain change delta. Pearson's correlation was not significant between variables $r = .593$, $p = .070$. **C**, Correlation analysis between time spent freezing during recall and pre-training prediction gain (PG) scores. There was not a significant correlation between pre-training PG and freezing during recall, $r = -.368$, $p = .295$. **D**, Correlational analysis between time spent freezing during recall and post-training PG scores. Spearman's rho did not reveal a significant correlation between post-training PG scores and freezing during recall, $rho = -.273$, $p = .488$. Error bars indicate SEM.

Figure 2—figure supplement 2. Modulation index changes across CFC and modulation index differences between sublayers.

A–C, Modulation indexes separated into discrete time windows: whole CFC recording, pre-shock baseline or post-shock windows. **A,** Modulation index for all CA1 neurons across three CFC windows (N = 264). A linear mixed-effects model revealed a significant main effect of window, $p < .001$. Post-hoc paired comparisons showed that modulation index was significantly higher during the pre-shock baseline than whole CFC, (Wilcoxon signed-rank, $p < .001$). Additionally, post-hoc comparisons significantly lower modulation index during the post-shock onset window than both whole CFC and pre-shock baseline, (Both, Wilcoxon signed-rank, $p < .001$). **B,** Modulation index for ACC neurons across three CFC windows (N = 271). A linear mixed-effects model revealed no significant main effect of window, $p = .140$, **C,** Modulation index for CA1 firing activity across three CFC windows for CA1 sublayers (CA1sup: N = 81; CA1deep: N = 61). Linear mixed effect ANOVA model revealed a significant main effect of window for CA1 sublayers, $p < .001$. In CA1sup, modulation index was significantly higher during pre-shock baseline than whole CFC and significantly lower during post-shock onset than both whole CFC and pre-shock baseline, all Wilcoxon signed-rank $p < .001$. In CA1deep, modulation index was also higher during pre-shock baseline than whole CFC, paired t-test $p = .009$, and lower during post-shock onset than both whole CFC, Wilcoxon signed-rank $p = .003$, and pre-shock baseline, Wilcoxon signed-rank $p = .008$. However, there was no significant main effect of sublayer, $p = .090$. Furthermore, Window × Sublayer interaction was also not significant, $p = .487$. Error bars indicate ± SEM.

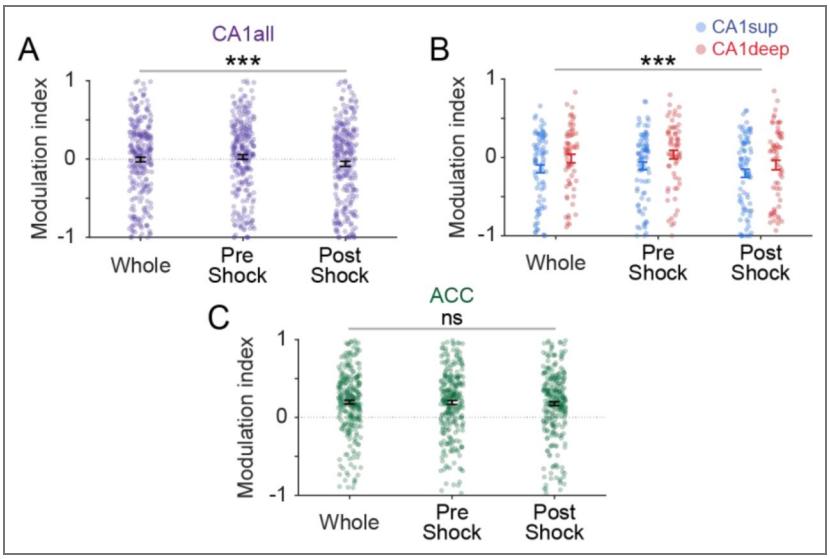

Figure 5—figure supplement 1. Representative histology for optogenetic experiments.

A, Optic fiber placement and ChR2 expression. **B,** Tetrode placement for CA1, arrow indicates location of tetrode tip.

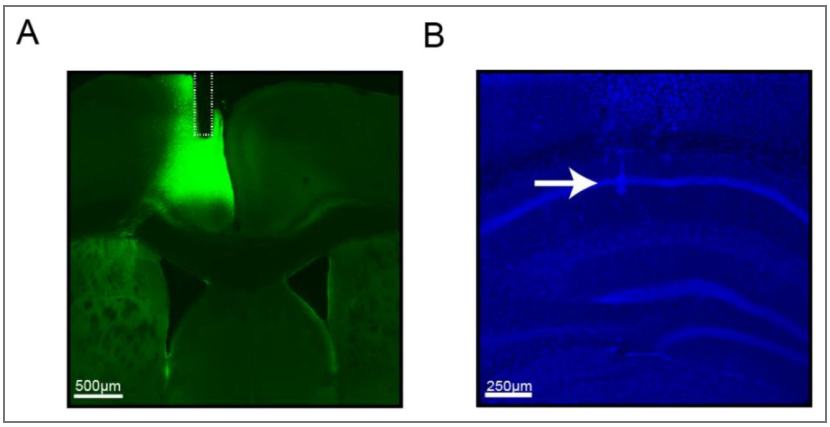

Figure 5—figure supplement 2. **CA1 neuron response to ACC stimulation,**

A, Heatmap for CA1sup neuron spiking (bin 20 ms) during wakefulness ACC stimulations (N = 94). **B,** Heatmap for CA1deepp neuron spiking (bin 20 ms) during wakefulness ACC stimulations (N = 34). Linear mixed effect model revealed no difference between CA1sublayers following ACC stimulation during wakefulness, p = .549.

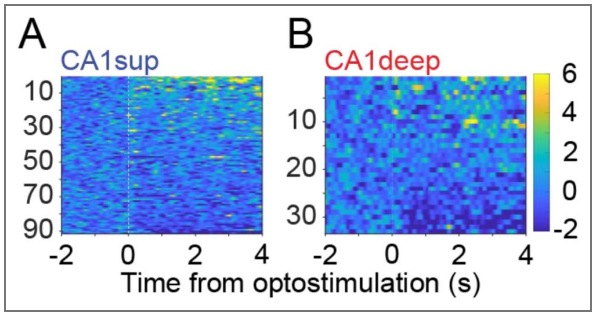

Figure 5—figure supplement 3.

A–E, Heatmaps for CA1 pyramidal neuron spiking (bin, 20 ms) separated per animal. **E,** Note, Animal 5 only had one recorded CA1sup neuron. That neuron was added to the CA1deep heatmap (Indicated by blue star).

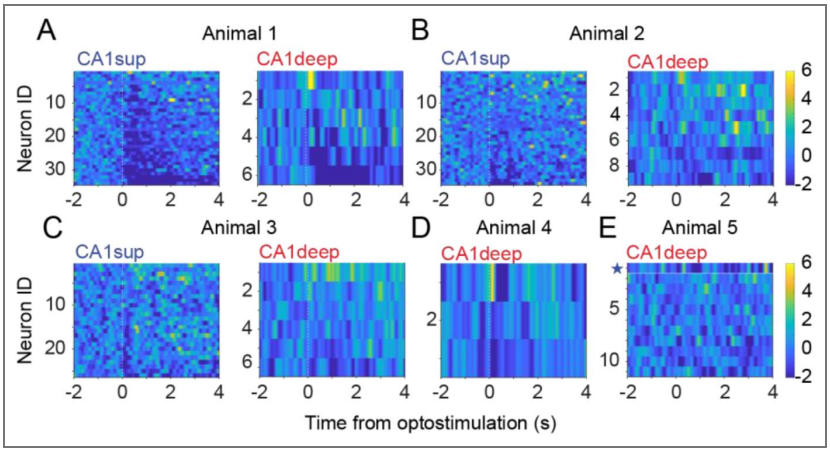

Figure 6—figure supplement 1. Putative Classifications of CA1 neurons.

A, Normalized waveform averaged across all recorded neurons for each neuron subtype in optogenetic stimulation studies (Pyramidal N = 130, PVs N = 17, V-type N = 17). **B,** Putative classifications of neurons based on neuron firing rate and spike width. **C,** Inter-spike interval for each neuron subtype. **D**, PV and V-type interneuron burst-index comparison. A two-sided Mann-Whitney U test revealed that PV neurons (N = 17) showed a significantly higher burst index than V-type neurons (N = 17), $p < .01$. Points indicate individual neurons; horizontal black lines indicate group medians and vertical black lines indicate interquartile ranges. E, Median response latency of significantly responsive neurons following ACC stimulation. Left, V-type interneuron had a median latency 10.5 ms (N = 11, IQR = 8.1–13.3 ms). Points indicate individual neurons; horizontal black lines indicate group medians and vertical black lines indicate interquartile ranges. Right, PV interneurons had a median latency of 97.5ms (N = 17, IQR = 37.5–295 ms). CA1sup neurons had a median latency to respond of 370 ms (N = 54, IQR = 130–830 ms). Points indicate median and horizontal lines interquartile ranges (IQR).

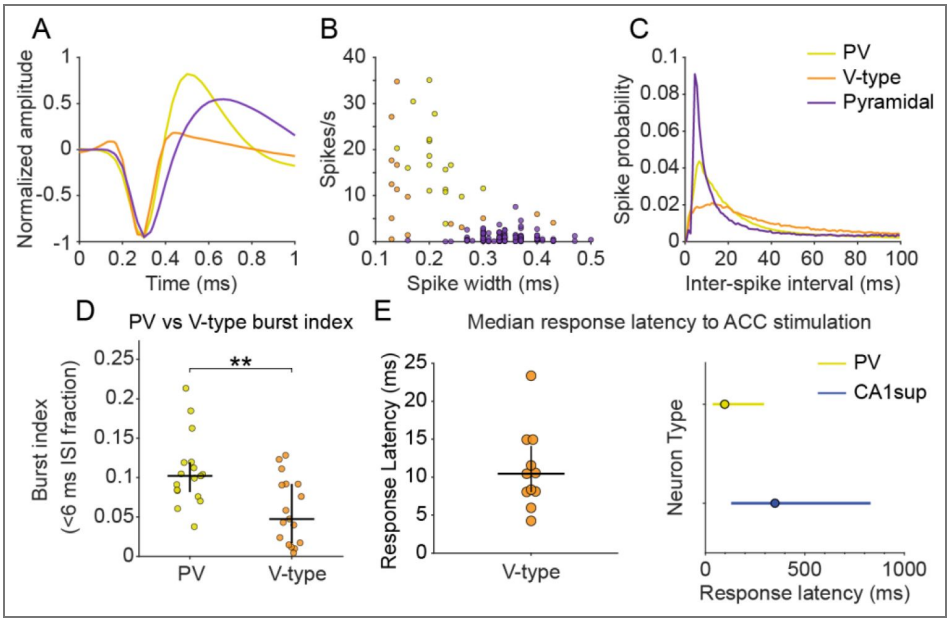

Figure 6—figure supplement 2. Per animal CA1 interneurons response to ACC stimulation,

A, Heatmap of PV interneuron activity following stimulation of the ACC (bin, 5 ms; N = 17). Colored spheres to the left of each row indicate animal identity. Neurons from the same animal share the same color. **B,** Heatmap of V-type interneurons spiking activity following stimulation of the ACC (bin, 1 ms; N = 17).

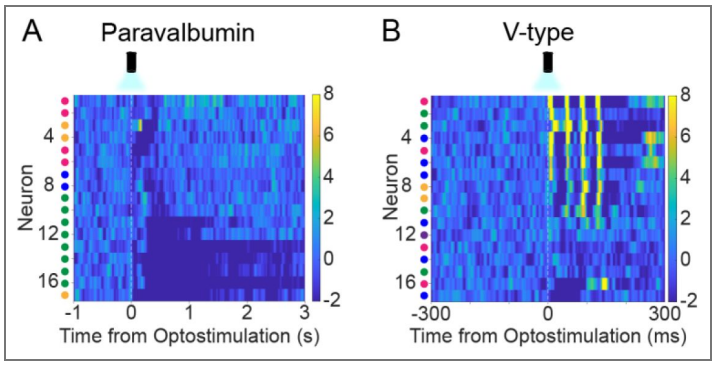

Data availability

Neural datasets, including all neural spiking and event timestamps, neuron waveforms, and local field potential recordings will be made publicly available on a public repository. Key customized MATLAB code used in the analysis will be available upon publication of this manuscript.

Acknowledgements

We thank the members of the Drexel ULAR staff for support and Dr. Wen-Jun Gao, Shayna Singh, Ashley Opalka, and Wenqiang Huang for their thoughtful comments.

Additional information

Author Contributions

AFH and DVW conceptualized the study. AFH performed all experiments. AFH and DVW wrote the manuscript.

Funding

This work was supported by NIH F31 MH134582 (AFH) and R01MH119102 (DVW).

Funding

Funder	Grant reference number	Author
HHS | NIH | National Institute of Mental Health (NIMH)	R01MH119102	Dong V Wang
HHS | NIH | National Institute of Mental Health (NIMH)	F31 MH134582	Arron F Hall

Author ORCID iDs

Dong V Wang: https://orcid.org/0000-0001-8537-5677

References

1. **Acsady L,** Halasy K, Freund TF (1993) Calretinin is present in non-pyramidal cells of the rat hippocampus--III. Their inputs from the median raphe and medial septal nuclei. *Neuroscience* **52**:829-841 https://doi.org/10.1016/0306-4522(93)90532-k | PubMed

2. **Anagnostaras SG,** Murphy GG, Hamilton SE, Mitchell SL, Rahnama NP, Nathanson NM, Silva AJ (2003) Selective cognitive dysfunction in acetylcholine M1 muscarinic receptor mutant mice. *Nat Neurosci* **6**:51-58 https://doi.org/10.1038/nn992 | PubMed

3. **Andrianova L,** Yanakieva S, Margetts-Smith G, Kohli S, Brady ES, Aggleton JP, Craig MT (2023) No evidence from complementary data sources of a direct glutamatergic projection from the mouse anterior cingulate area to the hippocampal formation. *eLife* **12**:e77364 https://doi.org/10.7554/eLife.77364 | PubMed

4. **Balduzzi D,** Tononi G (2013) What can neurons do for their brain? Communicate selectivity with bursts. *Theory in Biosciences* **132**:27-39 https://doi.org/10.1007/s12064-012-0165-0 | PubMed

5. **Behzadi G,** Kalén P, Parvopassu F, Wiklund L (1990) Afferents to the median raphe nucleus of the rat: Retrograde cholera toxin and wheat germ conjugated horseradish peroxidase tracing, and selectived</SPAN>-[^{3}H]aspartate labelling of possible excitatory amino acid inputs. *Neuroscience* **37**:77-100 https://doi.org/10.1016/0306-4522(90)90194-9 | PubMed

6. **Berndt M,** Trusel M, Roberts TF, Pfeiffer BE, Volk LJ (2023) Bidirectional synaptic changes in deep and superficial hippocampal neurons following in vivo activity. *Neuron* **111**:2984-2994.e2984. https://doi.org/10.1016/j.neuron.2023.08.014 | PubMed

7. **Buckner RL,** Andrews-Hanna JR, Schacter DL (2008) The brain's default network: anatomy, function, and relevance to disease. *Ann N Y Acad Sci* **1124**:1-38 https://doi.org/10.1196/annals.1440.011 | PubMed

8. **Buzsáki G** (2015) Hippocampal sharp wave-ripple: A cognitive biomarker for episodic memory and planning. *Hippocampus* **25**:1073-1188 https://doi.org/10.1002/hipo.22488 | PubMed

9. **Buzsáki G,** Horváth Z, Urioste R, Hetke J, Wise K (1992) High-frequency network oscillation in the hippocampus. *Science* **256**:1025-1027 https://doi.org/10.1126/science.1589772 | PubMed

10. **Castelli M,** Lopes-dos-Santos V, Gava GP, Lambiotte R, Dupret D (2025) Hippocampal Ripple Diversity organises Neuronal Reactivation Dynamics in the Offline Brain. *bioRxiv* https://doi.org/10.1101/2025.03.11.642571

11. **Cho JH,** Deisseroth K, Bolshakov VY (2013) Synaptic encoding of fear extinction in mPFC-amygdala circuits. *Neuron* **80**:1491-1507 https://doi.org/10.1016/j.neuron.2013.09.025 | PubMed

12. **Danielson NB,** Zaremba JD, Kaifosh P, Bowler J, Ladow M, Losonczy A (2016) Sublayer-Specific Coding Dynamics during Spatial Navigation and Learning in Hippocampal Area CA1. *Neuron* **91**:652-665 https://doi.org/10.1016/j.neuron.2016.06.020 | PubMed

13. **Davidson TJ,** Kloosterman F, Wilson MA (2009) Hippocampal replay of extended experience. *Neuron* **63**:497-507 https://doi.org/10.1016/j.neuron.2009.07.027 | PubMed

14. **DeLorey TM,** Handforth A, Anagnostaras SG, Homanics GE, Minassian BA, Asatourian A, Fanselow MS, Delgado-Escueta A, Ellison GD, Olsen RW (1998) Mice lacking the beta3 subunit of the GABAA receptor have the epilepsy phenotype and many of the behavioral characteristics of Angelman syndrome. *J Neurosci* **18**:8505-8514 https://doi.org/10.1523/jneurosci.18-20-08505.1998 | PubMed

15. **Diba K,** Buzsáki G (2007) Forward and reverse hippocampal place-cell sequences during ripples. *Nat Neurosci* **10**:1241-1242 https://doi.org/10.1038/nn1961 | PubMed

16. **Diekelmann S,** Born J (2010) The memory function of sleep. *Nat Rev Neurosci* **11**:114-126 https://doi.org/10.1038/nrn2762 | PubMed

17. **Ego-Stengel V,** Wilson MA (2010) Disruption of ripple-associated hippocampal activity during rest impairs spatial learning in the rat. *Hippocampus* **20**:1-10 https://doi.org/10.1002/hipo.20707 | PubMed

18. **Einarsson EÖ,** Nader K (2012) Involvement of the anterior cingulate cortex in formation, consolidation, and reconsolidation of recent and remote contextual fear memory. *Learning & Memory* **19**:449-452 https://doi.org/10.1101/lm.027227.112 | PubMed

19. **Esparza J,** Quintanilla JP, Cid E, Medeiros AC, Gallego JA, de la Prida LM (2025) Cell-type-specific manifold analysis discloses independent geometric transformations in the hippocampal spatial code. *Neuron* https://doi.org/10.1016/j.neuron.2025.01.022 | PubMed

20. **Fernández-Ruiz A,** Oliva A, Oliveira EF. d, Rocha-Almeida F, Tingley D, Buzsáki G (2019) Long-duration hippocampal sharp wave ripples improve memory. *Science* **364**:1082-1086 https://doi.org/10.1126/science.aax0758 | PubMed

21. **Foster DJ,** Wilson MA (2006) Reverse replay of behavioural sequences in hippocampal place cells during the awake state. *Nature* **440**:680-683 https://doi.org/10.1038/nature04587 | PubMed

22. **Frankland PW,** Bontempi B, Talton LE, Kaczmarek L, Silva AJ (2004) The Involvement of the Anterior Cingulate Cortex in Remote Contextual Fear Memory. *Science* **304**:881-883 https://doi.org/10.1126/science.1094804 | PubMed

23. **Freund TF,** Gulyas AI, Acsady L, Gorcs T, Toth K (1990) Serotonergic control of the hippocampus via local inhibitory interneurons. *Proc Natl Acad Sci U S A* **87**:8501-8505 https://doi.org/10.1073/pnas.87.21.8501 | PubMed

24. **Gava GP,** Lefèvre L, Broadbelt T, McHugh SB, Lopes-dos-Santos V, Brizee D, Hartwich K, Sjoberg H, Perestenko PV, Toth R, *et al.* (2024) Organizing the coactivity structure of the hippocampus from robust to flexible memory. *Science* **385**:1120-1127 https://doi.org/10.1126/science.adk9611 | PubMed

25. **Geiller T,** Fattahi M, Choi J.-S, Royer S (2017) Place cells are more strongly tied to landmarks in deep than in superficial CA1. *Nature Communications* **8**:1-11 https://doi.org/10.1038/ncomms14531 | PubMed

26. **Girardeau G,** Benchenane K, Wiener SI, Buzsáki G, Zugaro MB (2009) Selective suppression of hippocampal ripples impairs spatial memory. *Nature Neuroscience* **12**:1222-1223 https://doi.org/10.1038/nn.2384 | PubMed

27. **Girardeau G,** Inema I, Buzsáki G (2017) Reactivations of emotional memory in the hippocampus–amygdala system during sleep. *Nature Neuroscience* **20**:1634-1642 https://doi.org/10.1038/nn.4637 | PubMed

28. **Giri B,** Miyawaki H, Mizuseki K, Cheng S, Diba K (2019) Hippocampal Reactivation Extends for Several Hours Following Novel Experience. *J Neurosci* **39**:866-875 https://doi.org/10.1523/jneurosci.1950-18.2018 | PubMed

29. **Gridchyn I,** Schoenenberger P, O'Neill J, Csicsvari J (2020) Assembly-Specific Disruption of Hippocampal Replay Leads to Selective Memory Deficit. *Neuron* **106**:291-300.e296. https://doi.org/10.1016/j.neuron.2020.01.021 | PubMed

30. **Grosmark AD,** Buzsáki G (2016) Diversity in neural firing dynamics supports both rigid and learned hippocampal sequences. *Science* **351**:1440-1443 https://doi.org/10.1126/science.aad1935 | PubMed

31. **Gulati T,** Guo L, Ramanathan DS, Bodepudi A, Ganguly K (2017) Neural reactivations during sleep determine network credit assignment. *Nat Neurosci* **20**:1277-1284 https://doi.org/10.1038/nn.4601 | PubMed

32. **Halasy K,** Miettinen R, Szabat E, Freund TF (1992) GABAergic Interneurons are the Major Postsynaptic Targets of Median Raphe Afferents in the Rat Dentate Gyrus. *Eur J Neurosci* **4**:144-153 https://doi.org/10.1111/j.1460-9568.1992.tb00861.x | PubMed

33. **Hall AF,** Wang DV (2023) The two tales of hippocampal sharp-wave ripple content: The rigid and the plastic. *Progress in Neurobiology* **221**:102396 https://doi.org/10.1016/j.pneurobio.2022.102396 | PubMed

34. **Harris KD,** Hirase H, Leinekugel X, Henze DA, Buzsáki G (2001) Temporal interaction between single spikes and complex spike bursts in hippocampal pyramidal cells. *Neuron* **32**:141-149 https://doi.org/10.1016/s0896-6273(01)00447-0 | PubMed

35. **Harvey RE,** Robinson HL, Liu C, Oliva A, Fernandez-Ruiz A (2023) Hippocampo-cortical circuits for selective memory encoding, routing, and replay. *Neuron* **111**:2076-2090.e2079. https://doi.org/10.1016/j.neuron.2023.04.015 | PubMed

36. **Hefft S,** Jonas P (2005) Asynchronous GABA release generates long-lasting inhibition at a hippocampal interneuron-principal neuron synapse. *Nat Neurosci* **8**:1319-1328 https://doi.org/10.1038/nn1542 | PubMed

37. **Huang W,** Hall AF, Kawalec N, Opalka AN, Liu J, Wang DV (2026) *Anterior cingulate cortex in complex associative learning: monitoring action state and action content* In: eLife Sciences Publications, Ltd..

38. **Huang W,** Ikemoto S, Wang DV (2022) Median Raphe Nonserotonergic Neurons Modulate Hippocampal Theta Oscillations. *J Neurosci* **42**:1987-1998 https://doi.org/10.1523/JNEUROSCI.1536-21.2022 | PubMed

39. **Huelin Gorriz M,** Takigawa M, Bendor D (2023) The role of experience in prioritizing hippocampal replay. *Nature Communications* **14**:8157 https://doi.org/10.1038/s41467-023-43939-z | PubMed

40. **Jackson J,** Bland BH, Antle MC (2009) Nonserotonergic projection neurons in the midbrain raphe nuclei contain the vesicular glutamate transporter VGLUT3. *Synapse* **63**:31-41 https://doi.org/10.1002/syn.20581 | PubMed

41. **Jadhav SP,** Kemere C, German PW, Frank LM (2012) Awake Hippocampal Sharp-Wave Ripples Support Spatial Memory. *Science* **336**:1454-1458 https://doi.org/10.1126/science.1217230 | PubMed

42. **Jinde S,** Zsiros V, Jiang Z, Nakao K, Pickel J, Kohno K, Belforte Juan E, Nakazawa K (2012) Hilar Mossy Cell Degeneration Causes Transient Dentate Granule Cell Hyperexcitability and Impaired Pattern Separation. *Neuron* **76**:1189-1200 https://doi.org/10.1016/j.neuron.2012.10.036 | PubMed

43. **Karaba LA,** Robinson HL, Harvey RE, Chen W, Fernandez-Ruiz A, Oliva A (2024) A hippocampal circuit mechanism to balance memory reactivation during sleep. *Science* **385**:738-743 https://doi.org/10.1126/science.ado5708 | PubMed

44. **Karlsson MP,** Frank LM (2009) Awake replay of remote experiences in the hippocampus. *Nat Neurosci* **12**:913-918 https://doi.org/10.1038/nn.2344 | PubMed

45. **Karson MA,** Tang AH, Milner TA, Alger BE (2009) Synaptic cross talk between perisomatic-targeting interneuron classes expressing cholecystokinin and parvalbumin in hippocampus. *J Neurosci* **29**:4140-4154 https://doi.org/10.1523/jneurosci.5264-08.2009 | PubMed

46. **Kim EJ,** Pellman B, Kim JJ (2015) Stress effects on the hippocampus: a critical review. *Learn Mem* **22**:411-416 https://doi.org/10.1101/lm.037291.114 | PubMed

47. **Kim K.-R,** Kim Y, Jeong H.-J, Kang J.-S, Lee SH, Kim Y, Lee S.-H, Ho W.-K (2021) Impaired pattern separation in Tg2576 mice is associated with hyperexcitable dentate gyrus caused by Kv4.1 downregulation. *Molecular Brain* **14**:62 https://doi.org/10.1186/s13041-021-00774-x | PubMed

48. **Klausberger T,** Marton LF, Neill J, Huck JHJ, Dalezios Y, Fuentealba P, Suen WY, Papp E, Kaneko T, Watanabe M, *et al.* (2005) Complementary Roles of Cholecystokinin- and Parvalbumin-Expressing GABAergic Neurons in Hippocampal Network Oscillations. *The Journal of Neuroscience* **25**:9782 https://doi.org/10.1523/JNEUROSCI.3269-05.2005 | PubMed

49. **Klausberger T,** Somogyi P (2008) Neuronal diversity and temporal dynamics: the unity of hippocampal circuit operations. *Science* **321**:53-57 https://doi.org/10.1126/science.1149381 | PubMed

50. **Klinzing JG,** Niethard N, Born J (2019) Mechanisms of systems memory consolidation during sleep. *Nature Neuroscience* **22**:1598-1610 https://doi.org/10.1038/s41593-019-0467-3 | PubMed

51. **Lamotte G,** Shouman K, Benarroch EE (2021) Stress and central autonomic network. *Autonomic Neuroscience* **235**:102870 https://doi.org/10.1016/j.autneu.2021.102870 | PubMed

52. **Lee AK,** Wilson MA (2002) Memory of sequential experience in the hippocampus during slow wave sleep. *Neuron* **36**:1183-1194 https://doi.org/10.1016/s0896-6273(02)01096-6 | PubMed

53. **Lin L,** Chen G, Xie K, Zaia KA, Zhang S, Tsien JZ (2006) Large-scale neural ensemble recording in the brains of freely behaving mice. *J Neurosci Methods* **155**:28-38 https://doi.org/10.1016/j.jneumeth.2005.12.032 | PubMed

54. **Liu J,** Goto A, Hayashi Y (2024) Time-window of offline long-term potentiation in anterior cingulate cortex during memory consolidation and recall. *Neuroscience Research* https://doi.org/10.1016/j.neures.2024.12.009 | PubMed

55. **Liu J,** Hall AF, Wang DV (2024) Emerging many-to-one weighted mapping in hippocampus-amygdala network underlies memory formation. *Nature Communications* **15**:9248 https://doi.org/10.1038/s41467-024-53665-9 | PubMed

56. **Liu J,** Lin L, Wang DV (2021) Representation of Fear of Heights by Basolateral Amygdala Neurons. *J Neurosci* **41**:1080-1091 https://doi.org/10.1523/JNEUROSCI.0483-20.2020 | PubMed

57. **Liu Z.-W,** Faraguna U, Cirelli C, Tononi G, Gao X.-B (2010) Direct Evidence for Wake-Related Increases and Sleep-Related Decreases in Synaptic Strength in Rodent Cortex. *The Journal of Neuroscience* **30**:8671 https://doi.org/10.1523/JNEUROSCI.1409-10.2010 | PubMed

58. **Maris E,** Oostenveld R (2007) Nonparametric statistical testing of EEG- and MEG-data. *J Neurosci Methods* **164**:177-190 https://doi.org/10.1016/j.jneumeth.2007.03.024 | PubMed

59. **Masurkar AV,** Srinivas KV, Brann DH, Warren R, Lowes DC, Siegelbaum SA (2017) Medial and Lateral Entorhinal Cortex Differentially Excite Deep versus Superficial CA1 Pyramidal Neurons. *Cell Rep* **18**:148-160 https://doi.org/10.1016/j.celrep.2016.12.012 | PubMed

60. **Miettinen R,** Freund TF (1992) Convergence and segregation of septal and median raphe inputs onto different subsets of hippocampal inhibitory interneurons. *Brain Res* **594**:263-272 https://doi.org/10.1016/0006-8993(92)91133-y | PubMed

61. **Mizuseki K,** Diba K, Pastalkova E, Buzsáki G (2011) Hippocampal CA1 pyramidal cells form functionally distinct sublayers. *Nature Neuroscience* **14**:1174-1181 https://doi.org/10.1038/nn.2894 | PubMed

62. **Morales M,** Bloom FE (1997) The 5-HT3 receptor is present in different subpopulations of GABAergic neurons in the rat telencephalon. *J Neurosci* **17**:3157-3167 https://doi.org/10.1523/JNEUROSCI.17-09-03157.1997 | PubMed

63. **Norimoto H,** Makino K, Gao M, Shikano Y, Okamoto K, Ishikawa T, Sasaki T, Hioki H, Fujisawa S, Ikegaya Y (2018) Hippocampal ripples down-regulate synapses. *Science* **359**:1524-1527 https://doi.org/10.1126/science.aao0702 | PubMed

64. **Oh SW,** Harris JA, Ng L, Winslow B, Cain N, Mihalas S, Wang Q, Lau C, Kuan L, Henry AM, *et al.* (2014) A mesoscale connectome of the mouse brain. *Nature* **508**:207-214 https://doi.org/10.1038/nature13186 | PubMed

65. **Oliva A,** Fernández-Ruiz A, Leroy F, Siegelbaum SA (2020) Hippocampal CA2 sharp-wave ripples reactivate and promote social memory. *Nature* **587**:264-269 https://doi.org/10.1038/s41586-020-2758-y | PubMed

66. **Opalka AN,** Huang W.-q, Liu J, Liang H, Wang DV (2020) Hippocampal Ripple Coordinates Retrosplenial Inhibitory Neurons during Slow-Wave Sleep. *Cell Reports* **30**:432-441.e433. https://doi.org/10.1016/j.celrep.2019.12.038 | PubMed

67. **Papp EC,** Hajos N, Acsady L, Freund TF (1999) Medial septal and median raphe innervation of vasoactive intestinal polypeptide-containing interneurons in the hippocampus. *Neuroscience* **90**:369-382 https://doi.org/10.1016/s0306-4522(98)00455-2 | PubMed

68. **Petreanu L,** Huber D, Sobczyk A, Svoboda K (2007) Channelrhodopsin-2–assisted circuit mapping of long-range callosal projections. *Nature Neuroscience* **10**:663-668 https://doi.org/10.1038/nn1891 | PubMed

69. **Piñol RA,** Bateman R, Mendelowitz D (2012) Optogenetic approaches to characterize the long-range synaptic pathways from the hypothalamus to brain stem autonomic nuclei. *J Neurosci Methods* **210**:238-246 https://doi.org/10.1016/j.jneumeth.2012.07.022 | PubMed

70. **Raichle ME** (2015) The brain's default mode network. *Annu Rev Neurosci* **38**:433-447 https://doi.org/10.1146/annurev-neuro-071013-014030 | PubMed

71. **Rajasethupathy P,** Sankaran S, Marshel JH, Kim CK, Ferenczi E, Lee SY, Berndt A, Ramakrishnan C, Jaffe A, Lo M, *et al.* (2015) Projections from neocortex mediate top-down control of memory retrieval. *Nature* **526**:653-659 https://doi.org/10.1038/nature15389 | PubMed

72. **Ramanathan KR,** Maren S (2019) Nucleus reuniens mediates the extinction of contextual fear conditioning. *Behavioural brain research* **374**:112114 https://doi.org/10.1016/j.bbr.2019.112114 | PubMed

73. **Ramanathan KR,** Ressler RL, Jin J, Maren S (2018) Nucleus Reuniens Is Required for Encoding and Retrieving Precise, Hippocampal-Dependent Contextual Fear Memories in Rats. *The Journal of Neuroscience* **38**:9925 https://doi.org/10.1523/JNEUROSCI.1429-18.2018 | PubMed

74. **Ratigan HC,** Krishnan S, Smith S, Sheffield MEJ (2023) A thalamic-hippocampal CA1 signal for contextual fear memory suppression, extinction, and discrimination. *Nat Commun* **14**:6758 https://doi.org/10.1038/s41467-023-42429-6 | PubMed

75. **Raven F,** Aton SJ (2021) The Engram's Dark Horse: How Interneurons Regulate State-Dependent Memory Processing and Plasticity. *Front Neural Circuits* **15**:750541 https://doi.org/10.3389/fncir.2021.750541 | PubMed

76. **Rothschild G,** Eban E, Frank LM (2017) A cortical–hippocampal–cortical loop of information processing during memory consolidation. *Nature Neuroscience* **20**:251-259 https://doi.org/10.1038/nn.4457 | PubMed

77. **Senft RA,** Freret ME, Sturrock N, Dymecki SM (2021) Neurochemically and Hodologically Distinct Ascending VGLUT3 versus Serotonin Subsystems Comprise the r2-Pet1 Median Raphe. *J Neurosci* **41**:2581-2600 https://doi.org/10.1523/JNEUROSCI.1667-20.2021 | PubMed

78. **Sharif F,** Tayebi B, Buzsáki G, Royer S, Fernandez-Ruiz A (2021) Subcircuits of Deep and Superficial CA1 Place Cells Support Efficient Spatial Coding across Heterogeneous Environments. *Neuron* **109**:363-376.e366. https://doi.org/10.1016/j.neuron.2020.10.034 | PubMed

79. **Shi W,** Xue M, Wu F, Fan K, Chen QY, Xu F, Li XH, Bi GQ, Lu JS, Zhuo M (2022) Whole-brain mapping of efferent projections of the anterior cingulate cortex in adult male mice. *Mol Pain* **18**:17448069221094529 https://doi.org/10.1177/17448069221094529 | PubMed

80. **Silva BA,** Astori S, Burns AM, Heiser H, van den Heuvel L, Santoni G, Martinez-Reza MF, Sandi C, Gräff J (2021) A thalamo-amygdalar circuit underlying the extinction of remote fear memories. *Nature Neuroscience* **24**:964-974 https://doi.org/10.1038/s41593-021-00856-y | PubMed

81. **Souza R,** Bueno D, Lima LB, Muchon MJ, Gonçalves L, Donato J, Shammah-Lagnado SJ, Metzger M (2022) Top-down projections of the prefrontal cortex to the ventral tegmental area, laterodorsal tegmental nucleus, and median raphe nucleus. *Brain Struct Funct* **227**:2465-2487 https://doi.org/10.1007/s00429-022-02538-2 | PubMed

82. **Squire LR,** Genzel L, Wixted JT, Morris RG (2015) Memory consolidation. *Cold Spring Harbor perspectives in biology* **7**:a021766-a021766 https://doi.org/10.1101/cshperspect.a021766 | PubMed

83. **Szonyi A,** Mayer MI, Cserep C, Takacs VT, Watanabe M, Freund TF, Nyiri G (2016) The ascending median raphe projections are mainly glutamatergic in the mouse forebrain. *Brain Struct Funct* **221**:735-751 https://doi.org/10.1007/s00429-014-0935-1 | PubMed

84. **Tononi G,** Cirelli C (2003) Sleep and synaptic homeostasis: a hypothesis. *Brain Research Bulletin* **62**:143-150 https://doi.org/10.1016/j.brainresbull.2003.09.004 | PubMed

85. **Tononi G,** Cirelli C (2006) Sleep function and synaptic homeostasis. *Sleep Med Rev* **10**:49-62 https://doi.org/10.1016/j.smrv.2005.05.002 | PubMed

86. **Turi GF,** Li WK, Chavlis S, Pandi I, O'Hare J, Priestley JB, Grosmark AD, Liao Z, Ladow M, Zhang JF, *et al.* (2019) Vasoactive Intestinal Polypeptide-Expressing Interneurons in the Hippocampus Support Goal-Oriented Spatial Learning. *Neuron* **101**:1150-1165.e1158. https://doi.org/10.1016/j.neuron.2019.01.009 | PubMed

87. **Tzilivaki A,** Tukker JJ, Maier N, Poirazi P, Sammons RP, Schmitz D (2023) Hippocampal GABAergic interneurons and memory. *Neuron* https://doi.org/10.1016/j.neuron.2023.06.016 | PubMed

88. **Valero M,** Abad-Perez P, Gallardo A, Picco M, García-Hernandez R, Brotons J, Martínez-Félix A, Machold R, Rudy B, Buzsáki G (2025) Cooperative actions of interneuron families support the hippocampal spatial code. *Science* **389**:eadv5638 https://doi.org/10.1126/science.adv5638 | PubMed

89. **Valero M,** Cid E, Averkin RG, Aguilar J, Sanchez-Aguilera A, Viney TJ, Gomez-Dominguez D, Bellistri E, de la Prida LM (2015) Determinants of different deep and superficial CA1 pyramidal cell dynamics during sharp-wave ripples. *Nature Neuroscience* **18**:1281-1290 https://doi.org/10.1038/nn.4074 | PubMed

90. **Varga C,** Oijala M, Lish J, Szabo GG, Bezaire M, Marchionni I, Golshani P, Soltesz I (2014) Functional fission of parvalbumin interneuron classes during fast network events. *eLife* **3**:e04006 https://doi.org/10.7554/eLife.04006 | PubMed

91. **Wang DV,** Ikemoto S (2016) Coordinated Interaction between Hippocampal Sharp-Wave Ripples and Anterior Cingulate Unit Activity. *J Neurosci* **36**:10663-10672 https://doi.org/10.1523/jneurosci.1042-16.2016 | PubMed

92. **Wang DV,** Yau H.-J, Broker CJ, Tsou J.-H, Bonci A, Ikemoto S (2015) Mesopontine median raphe regulates hippocampal ripple oscillation and memory consolidation. *Nature Neuroscience* **18**:728-735 https://doi.org/10.1038/nn.3998 | PubMed

93. **Wang J,** Hasan MT, Seung HS (2009) Laser-evoked synaptic transmission in cultured hippocampal neurons expressing channelrhodopsin-2 delivered by adeno-associated virus. *J Neurosci Methods* **183**:165-175 https://doi.org/10.1016/j.jneumeth.2009.06.024 | PubMed

94. **Watson Brendon O,** Levenstein D, Greene JP, Gelinas Jennifer N, Buzsáki G (2016) Network Homeostasis and State Dynamics of Neocortical Sleep. *Neuron* **90**:839-852 https://doi.org/10.1016/j.neuron.2016.03.036 | PubMed

95. **Wilson MA,** McNaughton BL (1994) Reactivation of hippocampal ensemble memories during sleep. *Science* **265**:676-679 https://doi.org/10.1126/science.8036517 | PubMed

96. **Xu W,** Südhof TC (2013) A Neural Circuit for Memory Specificity and Generalization. *Science* **339**:1290-1295 https://doi.org/10.1126/science.1229534 | PubMed

Hall AF, Wang DV (2026) A cortical-hippocampal communication undergoes rebalancing after new learning. A cortical-hippocampal communication undergoes rebalancing after new learning. figsahre. https://doi.org/10.6084/m9.figshare.33467404.v2

Peer reviews

Reviewer #2 (Public review):

This work is composed of two largely independent parts. The first part (Figures 1-4) attempts to study correlations between the anterior cingulate cortex (ACC) and hippocampal area CA1 in the context of learning and memory; a number of issues including missing controls make this part inconclusive and hard to interpret. The second part (Figures 5 and 6) presents evidence for a pathway in which inputs from the ACC indirectly inhibit pyramidal cells in the superficial sublayer of CA1. The optogenetic evidence demonstrating the functional connection, including the interneurons likely to be involved, is convincing, making the second part of the manuscript a valuable contribution to neuroscience. However, I do not see evidence for this connection in the correlational analyses in the first part of the study, making the involvement of this pathway in learning and memory uncertain.

Strengths:

The biggest strength of the work is the optogenetic manipulation experiments in the second part of the study (Figures 5 and 6), which convincingly demonstrate that stimulation of ACC pyramidal neurons activates an interneuron population with symmetric spike waveforms, and inhibits parvalbumin interneurons and pyramidal cells in CA1sup, while CA1deep cells remained largely unaffected by the stimulation.

Weaknesses:

The main weakness is the disconnected nature of the two parts of the study. The second part convincingly shows that ACC provides a net inhibitory drive to the hippocampus (at least to CA1sup pyramidal and PV cells, while CA1deep cells were mostly unaffected). However, the first part investigates positive cross-correlations between pre-ripple ACC activity and subsequent CA1 ripple activity. This can be observed in Figure 1-supplement 1, where CA1 cells' activity peaks around 70ms after ACC spikes. Moreover, the GLM analyses were also based on positive ACC cell-CA1 cell pair correlations as the authors reported no bias towards negative weights for the GLM analyses (see the rebuttal letter). Thus, the correlational and GLM analyses in the first part primarily characterize a positive ACC-CA1 relationship, rather than the inhibitory influence demonstrated in the second part; the two parts of the manuscript therefore investigate different phenomena (possibly confounding inputs and network effects in part 1 versus the direct ACC-CA1 connection in part 2).

The key problem is that the main results of the two parts - namely, a dampening of the positive cross-correlations following learning in part 1 and the inhibitory ACC-CA1 connection revealed in part 2 - would be contradictory if they were interpreted as describing the same phenomenon. If the inhibitory ACC-CA1 connection was key to the downregulation of CA1 activity after learning as the authors suggest in the discussion, then we would expect ACC activity driving this change to be particularly predictive of CA1 activity in this post-

learning period. Indeed, because prediction gain measures how well ACC spiking can predict subsequent CA1 spiking, any additional predictive information from the direct ACC->CA1 pathway should increase prediction gain. Instead, prediction gain decreased following learning. Thus, the positive (dampened after learning) ACC-CA1 correlations observed in the first part cannot be explained by the inhibitory ACC-CA1 pathway demonstrated in the second part. The most likely explanation is therefore that the cross-correlations studied in part 1 are dominated by other factors (such as shared inputs from other areas or coordination of cortical rhythms) and reported changes in prediction gain therefore primarily reflect changes in these factors, while the contribution of the direct ACC-CA1 pathway is drowned out and undetectable using this approach. As they stand, the two halves of the paper cannot be reconciled into the same framework.

The second weakness is the lack of control for learning. The main result of part 1 of the study is that there is dampening of the (positive) CA1 response to ACC pre-ripple activity after learning. However, nothing indicates this is due to learning as there is no control data with no learning. Moreover, the pre- and post- task periods were not matched for duration and sleep depth, so it is entirely possible that the observed dampening could be due to reduced recruitment of some cells in ripples. An appropriate control would therefore be important for attributing this to learning

The final weakness is statistical and goes beyond the lack of hierarchical statistics (which is also an issue with this work). The failure of a test to reach significance cannot be interpreted as evidence for the opposite. Yet the authors interpret it as such: for example, the lack of significant correlation between prediction gain values in pre- and post-task sleep in Figure 3C ($p=0.14$) is incorrectly interpreted as proof that ACC-CA1sup communication has reorganized as a result of learning. The claims of reorganization (mentioned multiple times in the abstract) hinge solely on this failed statistical test. Yet a failure to reach significance does not successfully demonstrate reorganization as it could result from a number of other reasons, including lack of statistical power or noisy estimates. To demonstrate reorganization, one would need to show that the observed change is greater than expected under an appropriate control (e.g. control task with no learning; or sleep data split in two halves), but this is missing from this manuscript.

Note that in the entire manuscript, the only differences between CA1sup and CA1deep are reported as two independent tests, one of which is significant and the other does not reach statistical significance. However, this is not evidence for different effects in CA1sup and CA1deep and statements like "we uncovered a pathway-specific difference" to describe these findings are unwarranted and not supported by the data; only direct statistical comparison between the two effects could support such claims. The exception to this weakness is the optogenetic experiments in Figure 5 where CA1sup and CA1deep responses to optogenetic ACC stimulation were directly compared and found to be different.

https://doi.org/10.7554/eLife.107370.2.sa1

Author response:

The following is the authors' response to the original reviews.

> ***Public Reviews:***
>
> ***Reviewer #1 (Public review):***
>
> *Summary:*
>
> *This work by Hall et al provides a novel and important new finding about communication between the anterior cingulate cortex (ACC) and the CA1 region of the dorsal*

> *hippocampus: there is a clear ability of ACC to predict CA1 activity, and that is modulated by learning/experience. Furthermore, they have some evidence that the modulation differs by whether the CA1 neurons were in the deep versus superficial sub-layer of CA1. The evidence is suggestive of new and exciting findings, but some gaps and weaknesses remain to be addressed before I believe all of the authors' claims can be supported. The figures also need to be slightly better organized, and the discussion is missing a major dimension in my opinion. Overall, this is a strong submission, but with some gaps to fill.*
>
> *Strengths:*
>
> *(1) This is a well-written manuscript - the introduction was especially clear, well-cited, and motivating.*
>
> *(2) The sub-layer specific communication between ACC and CA1 represents the discovery of a novel and functionally impactful piece of neurobiology.*
>
> *(3) Optogenetics was an important verification of ACC-CA1 communication, as was the analysis of neurons by waveform type.*
>
> *Weaknesses:*
>
> *(1) Figure 2: Why are the data separated into two groups from the outset? If all data are combined, is there a general drop in prediction gain from pre to post?*

Thank you for bringing this to our attention. In Figure 1F, all data is combined for GLM decoding. We found a significant pre-to-post decrease in prediction gain specifically using the –200 to 0 ms window to predict CA1 spiking during ripples. Figure 3 builds upon these findings to examine how prediction gain changes relate to task engagement.

> *(2) 2b and 2c are important since they are complementary means to show the same thing, and it is important that they cross-validate each other, especially since the non-significant task active neuron difference in 2b appears to be nearly as strong as the significant difference to its left. A more holistic analysis can be done to compare these dimensions.*

We appreciate this feedback. In light of this comment, as well as similar concerns raised by other reviewers regarding the binary classification of neurons as task-active or task-inactive (modulation index > 0 or < 0), we adopted a more comprehensive analytical approach. Rather than relying on an arbitrary threshold, we first examined the continuous relationship between modulation index and prediction gain change across all neurons (Figure 2C). We then divided neurons into modulation index quartiles to assess whether prediction gain changes varied across different degrees of task modulation (Figure 2D). Follow-up analyses focused on the extreme quartile comparisons that contributed to the observed effects (Figure 2E). Overall, this new approach better captured the continuous nature of task-related modulation while avoiding the inclusion of a large population of neurons with modulation indices near zero that may not meaningfully differ in task engagement. However, we were unable to replicate modulation index changes for neurons split by prediction gain score percentile and removed those figures from the manuscript. We have adjusted the text accordingly to account for this new effect.

> *(3) Sup vs deep neuron definition: Did the authors have any means to validate this anatomical separation using histology or otherwise? I don't believe they described anything like that, and instead use physiology to infer anatomical location. I understand anatomy-based methods may be practically impossible with tetrodes, but this limitation should at least be mentioned, and it should be explained that without something like silicon probes or histological validation, anatomy had to be inferred from physiology.*

We think this is an important limitation to address and thank you for bringing this to our attention. Given our technical restraints, we only validated radial position through physiological properties. This remains an outstanding limitation of this study. We have since added text into the main discussion bringing attention to this limitation. See below:

“Lastly, our CA1 sublayer classification does come with its own caveats. Tetrode identification of CA1 sublayers is not a trivial matter. We implemented guidelines informed by past research (see methods) to help ensure we isolated CA1sup and CA1deep groups, only including neurons where we had the greatest confidence (Berndt et al., 2023; Mizuseki et al., 2011). In doing so, we excluded neurons which classification was uncertain. It is possible this excludes some meaningful populations of CA1 sublayers. Additionally, despite our approach, some cross-inclusion of sublayers may remain. Therefore, interpretations of CA1 sublayers difference should be considered with these limitations in mind. That said, the number of neurons and animals tested does provide overall confidence regarding our results. Future studies investigating this ACC to CA1 sublayer specific line of communication would benefit from the use of silicon probes or neuropixels that enable precise radial localization.”

> *(4) Superficial vs deep differences in firing rate ratio based on PG: there are many fewer CAdeep neurons, but in 4c, the trends appear to be the same pre-training, top PG lower than others. It seems the lack of difference in CA1deep in 4c may be due to the much lower power/n. This should be discussed or addressed.*

We appreciate this feedback and since have added more recordings to address these lower Ns (CA1sup: Previous N = 71, Revisions N = 89; CA1deep: Previous N = 21, Revisions N = 61). Notably, we find that previous firing rate ratio (now called modulation index) is no longer significant with the inclusion of more neurons and is reported accordingly (Figure 2—figure supplement 1).

> *(5) In Figure 5, the term "firing rate ratio" is used, and it sounds the same as in previous figures, but this is a different ratio (based on modulation by opto stim, not task).*

To improve clarity and avoid confusion with task-related modulation metric used across the paper, we renamed “Firing Rate Ratio" throughout the manuscript to "Modulation Index". We also relabeled the Figure 5D Y-axis as "Z-scored Firing Response" to more accurately reflect the plotted data and avoid confusion.

> *(6) I would like to learn more about these v-type neurons. I understand we do not yet know about their molecular or morphologic correlate, but more analysis can be done with the current data.*

We thank you for this feedback. We have included further analysis into V-type properties. Namely, we performed autocorrelegrams, theta phase modulation, and burst index analyses. See Figure 6 and Figure 6—figure supplement 1.

Additionally, we performed cross-correlogram analyses to examine whether V-type interneurons exhibited consistent temporal relationships with PV interneurons or other CA1 neurons. However, V-type and PV interneurons were sparse throughout our recordings, with most sessions containing two or fewer identified interneurons, which limited our ability to perform meaningful cross-correlogram analyses. Nevertheless, we examined the available recordings but found no consistent evidence of correlated firing between interneuron classes or between V-type interneurons and CA1 pyramidal neurons.

> *(7) I would like more discussion of ACC-CA1 connectivity.*

We have since added greater discussion of ACC-CA1 connectivity into the discussion section. See below:

"Finally, an important caveat to mention is that it remains an ongoing debate whether ACC directly projects to CA1 (Andrianova et al., 2023; Rajasethupathy et al., 2015; Shi et al., 2022). One lab reported clear monosynaptic ACC-to-CA1 connection (Rajasethupathy et al., 2015), while another lab replicated those same experiments and were unable to come to the same conclusions (Andrianova et al., 2023). Further studies report no direct connection (Shi et al., 2022). The contention in connectivity may arise from differences in targeting strategies, injection coordinates, or viruses used. Our findings reported an excitatory response in CA1 V-type interneurons in response to ACC stimulations, proposing another possibility for ACCàCA1 connectivity. Interestingly V-type interneurons responded with extremely low-latency as fast as 4.2 ms after stimulations, compatible with monosynaptic timing (Cho et al., 2013; Petreanu et al., 2007; Wang et al., 2009). If the ACC→V-Type connection was monosynaptic pathway, it could help explain discrepancies in the field, as the relative sparsity of V-type interneurons may reduce the likelihood of detecting ACC→CA1 connectivity. However, future anatomical studies are needed to conclusively determine connectivity.

Alternatively, ACC→CA1 communication may be mediated by multiple intermediate structures (Behzadi et al., 1990; Oh et al., 2014; Shi et al., 2022; Souza et al., 2022). The ACC sends monosynaptic projections to the nucleus reuniens (RE) and median raphe (MnR), both of which project directly to CA1 (Oh et al., 2014; Shi et al., 2022). The RE has a known role in contextual discrimination learning and memory specificity (Ramanathan & Maren, 2019; Ramanathan et al., 2018; Ratigan et al., 2023; Silva et al., 2021; Xu & Südhof, 2013). Interestingly, RE→CA1 activity tuned to immobility (freezing) emerges only after shocks are presented, suggesting a learning-induced modification between regions, similar to that seen in our ACC–CA1 data (Ratigan et al., 2023). As for MnR, it receives dense inputs from the ACC (Behzadi et al., 1990; Souza et al., 2022), and its projections to the CA1 are predominantly glutamatergic (Jackson et al., 2009; Senft et al., 2021; Szonyi et al., 2016). Notably, these glutamatergic MnR inputs directly target CA1 interneurons, including CCK basket cells (Miettinen & Freund, 1992; Morales & Bloom, 1997; Senft et al., 2021), while avoiding PV interneurons and pyramidal neurons (Acsady et al., 1993; Freund et al., 1990; Halasy et al., 1992; Miettinen & Freund, 1992; Papp et al., 1999; Turi et al., 2019). This connectivity suggests that the ACC may indirectly modulate CA1 activity through the MnR, potentially suppressing PV interneuron and pyramidal neuron activity via local inhibitory circuits, thereby contributing to the regulation of hippocampal oscillations and memory consolidation (Huang et al., 2022; Wang et al., 2015). Ultimately, future experiments combining pathway-specific manipulations with simultaneous recordings will be necessary to distinguish direct from polysynaptic mechanisms."

> *(8) Some elements may be missing from the discussion, relating baseline functioning versus post-learning function.*

We thank the reviewer for this feedback and their recommendation for possible alternate explanations. We have added these discussions into the main text. See below:

"Alternatively, ACC→CA1 communication may contribute to the homeostatic downscaling of memory-unrelated synapses during sleep. Evidence finds that slow-wave sleep is strongly linked to downscaling of non-learning related neuron activity (Gulati et al., 2017; Liu et al., 2010; Tononi & Cirelli, 2003; Tononi & Cirelli, 2006; Watson et al., 2016). Slow-wave sleep ripples in particular depotentiate memory-unrelated synapses (Gulati et al., 2017; Norimoto et al., 2018). In our study, we find that learning-related reduction in communication between ACC and CA1 were selective for task-inactive neurons. Therefore, ACC→CA1sup communication may not simply weaken following learning but rather becomes selectively disengaged from task-inactive neurons, enabling homeostatic downscaling while preserving behaviorally relevant synapses (Liu et al., 2010; Norimoto et al., 2018; Tononi & Cirelli, 2003; Tononi & Cirelli, 2006; Watson et al., 2016). Still, behavioral recruitment alone cannot account

for the observed remodeling of ACC→CA1 communication, as CA1sup and CA1deep neurons did not display significant differences in task-related activity (Figure 2—figure supplemental 2). Instead, these learning-related changes of task-inactive neurons appear sublayer-specific."

> ***Reviewer #2 (Public review):***
>
> *Summary:*
>
> *This study uncovers an inhibitory pathway from the anterior cingulate cortex (ACC) to pyramidal cells in the superficial sublayer of hippocampal area CA1 (CA1sup). As ACC neuron spiking tends to precede hippocampal ripples, this presents the intriguing possibility that ACC inputs are selectively inhibiting particular CA1sup neurons, which could play a role in the reactivation of task-related ensembles known to take place during hippocampal ripples. Indeed, through a generalized linear model (GLM) analysis, the authors demonstrate that the ACC activity within the 200ms immediately preceding the ripple is predictive of the ripple content.*
>
> *Strengths:*
>
> *The biggest strength of the work is the optogenetic manipulation experiments, which convincingly demonstrate that stimulation of ACC pyramidal neurons activates an interneuron population with symmetric spike waveforms, and inhibits parvalbumin interneurons and pyramidal cells in CA1sup but not CA1deep sublayer.*
>
> *An additional strength in the GLM analysis which consistently shows that ACC activity preceding the ripple is predictive of hippocampal activity during the ripple considerably more than in shuffled data for all cells and periods tested.*
>
> *Weaknesses:*
>
> *The major weakness of this work is that the link with learning and memory is not very well supported.*
>
> *The only evidence of rebalancing and reorganization appears to be a single statistical test (the test in Figure 1f, p=0.013) demonstrating a decrease of the GLM prediction gain from pre-task sleep to post-task sleep; the same test is repeated for subsets of the data in the rest of the figures. As the idea of rebalancing and reorganization is central to the paper as currently written, exploring it through another measure, independent of the GLM prediction gain, should be expected. The notion that this pathway is suppressed in sleep following learning can be supported by demonstrating a decrease in any of the following measures: ACC spike-triggered average CA1sup responses, cross-covariances (Wierzynski et al 2009) between ACC and CA1sup cells in post-task sleep, or ripple-triggered cross-correlations (Sirota et al. 2009).*

We thank the reviewer for this helpful feedback. We have added an additional analysis the reviewer pointed out to address this concern. Specifically, we performed an ACC spike-triggered analysis. The ACC spike-triggered average further supported the learning-related decrease in ACC-to-CA1 activity (see Figure 1—figure supplement 1). We did not include a separate cross-covariance analysis because the ACC spike-triggered average captures essentially the same temporal relationship between ACC and CA1 activity.

> *The differences between task-active and task-inactive neurons are not convincing. The separation between task-active and task-inactive neurons is to divide a distribution that is far from bimodal into what appears to be two arbitrary groups. Similarly, the authors divide cells relative to their prediction gain ("Top PG" and "Bottom PG" in Figure 2c), which fails to select for the population of significantly predicted cells (relative to the shuffle). Within CA1sup cells, after learning, there is a significant decrease in the*

> *prediction gain for "task-inactive" cells but not "task-active" cells, but it is important to keep in mind that the "task-active" group contains only 24 neurons, and there was no difference between the two groups of cells ("task-active" vs "task-inactive") when directly compared.*

We agree with this concern. To address this, we removed conclusion based on those arbitrary criteria instead opting for a more continuous approach. Specifically, we adopted a more comprehensive analytical approach. Rather than relying on an arbitrary threshold, we first examined the continuous relationship between modulation index and prediction gain change across all neurons (Figure 2C). We then divided neurons into modulation index quartiles to assess whether prediction gain changes varied across different degrees of task modulation (Figure 2D). Follow-up analyses focused on the extreme quartile comparisons that contributed to the observed effects (Figure 2E). Overall, this new approach better captured the continuous nature of task-related modulation while avoiding the inclusion of a large population of neurons with modulation indices near zero that may not meaningfully differ in task engagement.

> *Finally, it is not clear whether the identity of the pathway-responsive CA1sup neurons is fixed or whether it may change with learning. A deeper analysis into the cell pair cross-correlations or the weights of the GLM analysis may reveal whether there is a reorganization of CA1sup responses (some cells that were inhibited are no longer inhibited, and vice versa) or a dampening (the same CA1sup cells are inhibited in both cases, but the inhibition is less-pronounced in post-task sleep). The possibility of a rigid circuit dampened immediately following fear conditioning, is not discussed by the authors.*

We appreciate this feedback. To address this concern without weight analysis, we examined the stability of prediction gain scores between pre- and post-training sleep. Preservation of neuronal prediction-gain rankings would suggest that learning weakens existing predictive communication while maintaining the relative contribution of individual neurons, consistent with a dampening response. In contrast, poor preservation of prediction-gain rankings would be more indicative of a reorganization of predictive relationships across the population. This led to interesting findings regarding sublayer differences: ACC→CA1sup communication is more dynamic and evolving following learning, whereas ACC→CA1deep communication remains comparatively stable (See Figure 2A&B; Figure 3 C–F).

> ***Reviewer #3 (Public review):***
>
> *Summary:*
>
> *In this study, Hall and colleagues investigate how the coupling of activity from ACC to CA1is altered by fear learning, showing that during sleep immediately before learning, there is evidence for increased coupling of ACC activity with neurons that will subsequently be inhibited during the learning process. They go on to show that this effect seems to be mediated most by a subpopulation of neurons in the superficial layer of CA1. This fits with previous reports suggesting that these superficial neurons are key for the flexible updating of memory. The authors then go on to show that artificial activation of ACC using optogenetics results in varied effects in CA1, including a subtle decrease in activity of superficial neurons that lasts longer than the stimulus itself. Finally, the authors present some preliminary data suggesting that different interneurons may be recruited by this optogenetic stimulation in different ways and at different times.*
>
> *Overall, this is an interesting paper, but much of the analysis is very preliminary, and much of the crucial data about the learning effects and alterations to cell firing are not presented clearly and fully. This is further confounded by a rather opaque description of the results and analysis in the text. Overall, there is something very interesting here, but*

> *there needs to be a substantial series of extra analyses to clearly say what this is. In many cases, more robust analysis may render the results underpowered, which could dramatically change the conclusions of the paper.*
>
> *Strengths:*
>
> *The authors performed difficult, dual-location recordings across a multi-day learning paradigm, which seems like it could be a really nice dataset. They delve into the circuit basis of an interesting finding regarding ACC to CA1 connectivity and how this changes before and after fear conditioning. They provide data to suggest this connectivity may be through specific and distinct subcircuits in CA1.*
>
> *Weaknesses:*
>
> *(1) There is essentially no information in the text or figures about what the actual learning was, how it was done, how individual animals performed, and how any of these metrics related to learning. Looking at the methods, the authors did a number of things never mentioned anywhere in the text or figures, including novel arena exposure, contextual reexposure in extinction after learning, etc. It seems that this is a very rich dataset that has not been presented at all. I would recommend at the very least:*

We appreciate the reviewers' feedback and have worked to address these concerns. See below our response.

> *(a) Plot all of the behavioural training data, and how each mouse relates to one another - did the mice learn? At this stage, we don't know!*

We have now plotted all contextual fear conditioning behavioral data for each mouse (Figure 2—figure supplement 1). All mice exhibited high level of freezing during the contextual fear test, suggesting successful learning of the context–shock association.

> *(b) Explain in the text in detail exactly what was done and why, and what this tells us about the neuronal activity.*

We have now added text to describe in detail the behavioral results and how that may relate to our GLM analyses. We have also more clearly detailed our experimental objectives (what was done and why) utilizing contextual fear conditioning,

"In this approach, we were able to examine ACC–CA1 communication prior, during, and after learning, enabling us to examine how this communication evolves across fear learning. Specifically, we emphasized investigation into communication changes between pre- and post-training sleep to understand whether functional connectivity undergoes learning-related reorganization."

"Lastly, we examined whether PG scores correlated with the freezing response in mice during recall. Across all mice, freezing was significantly higher during recall than pre-shock baseline during training (Figure 2—figure supplement 2A). Overall, we found no correlation between PG and freezing (Figure 2—figure supplement 2B–D). However, there was a trend for a positive correlation ($p = .07$) between ΔPG and freezing percentage. An important consideration is that the uniformly high levels of freezing in mice limited behavioral variability, potentially reducing our ability to detect relationships between ACC–CA1 communication decoding and behavioral differences."

> *(c) If there is variance in learning and or conditioning, does this relate to features in the analysis, such as the GLM result.*

We examined this question by first investigating whether prediction gain scores in pre-training, post-training, or overall ΔPG correlated with freezing percentage. We found no

significant correlation between any of the variables (Figure 2—figure supplement 1). We speculate this may be a result of a relatively robust freezing response limiting the ability for our fine-grained GLM decoding analyses to detect those differences. We have added this consideration to the main text.

> *(2) Along similar lines, a key metric for most of the paper is that neurons most coupled with ACC are more likely to be inhibited during training. However, there is nothing anywhere in the paper showing these data. How do neurons in general respond to contextual shocks? The methods describe this as the average firing rate during training, normalised to pre-sleep activity. This metric seems a bit coarse and may obscure really important task-relevant dynamics. Are the neurons active at specific times, are they tuned to relevant parts of the task, and do any of these features of the cell activity also relate to the coupling with ACC? Similarly, how did the authors mitigate the influence of electrical artefacts caused by the foot shock in their recordings? Again, there is a huge amount of data here that is not being described, and likely holds very valuable information about what is actually happening. The paper would really benefit from the inclusion of these data in an accessible form, such as heatmaps of spiking, how these patterns change over time, and around e.g., foot shock, etc. Also key is how these features are altered by the variability of learning across subjects.*

We thank reviewer for this feedback. As pointed out, electrical artifacts caused by the footshocks prevents our ability to examine, with temporal sensitivity, neurons' responses to footshocks. Therefore, we are left to examine activity changes across longer timescales. We acknowledge that our current modulation index analysis is a bit coarse. One reason is that our preliminary analyses using more temporally sensitive approaches did not reveal robust CA1 activity associated with specific behaviors, such as freezing or transitions between mobility and immobility. Thus, we chose a more holistic approach looking at the full CFC session to include all components that CA1 may be encoding during the training session. For example, although the pre-shock baseline period does not contain any footshock stimuli, it serves a key part in the process as mice begin to encode their environment around them. Nevertheless, we have added an additional analysis to examine how modulation changes across the pre-shock versus post-shock window (Figure 5—figure supplement 1). Although this provides greater insight into how ACC and CA1 activity changes across different dimensions in the task, further investigation utilizing casual manipulations is necessary to elucidate which phase ACC→CA1 activity is most involved.

> *(3) A number of the effects are presented by comparing a statistically significant effect to a non-statistically significant effect (e.g. in Figure 2b, Figure 2d, Figure 4 b,c, and others). This isn't really valid - the key test that the two groups are different is either with a direct test of the difference or an interaction term in an e.g., ANOVA test. In some places, I am not sure the same conclusions will be drawn from the data with these tests.*

We want to thank the reviewer for this critical feedback. We have since added the appropriate statistical measure including linear mixed-effects models and ANOVA tests and for our analysis to avoid our previous statistical errors.

> *(4) To what extent is defining superficial and deep CA1 neurons solely by ripple waveform an accepted method? Of the two papers referenced for this approach, one is a 2-photon calcium imaging paper that does not do electrical recordings (as far as I am aware), and the second uses this as a descriptor after defining the positions of units on an array. It would be good to clarify how accepted this is, and also how robust this is. At the very least, some kind of metric or walkthrough in the supplement as to how this was done, and how well each cell was classified and with what confidence, or some metric of how distinct and separate the two populations were (or was it just a smudge).*

We appreciate this feedback. While the Berndt 2023 paper implemented 2-photon calcium imaging, they also used tetrode classifications for radial axes in that paper which help informed our approach. Ultimately, our tetrode classification remains an outstanding limitation which we have since added to the main text (See below).

“Lastly, our CA1 sublayer classification does come with its own caveats. Tetrode identification of CA1 sublayers is not a trivial matter. We implemented guidelines informed by past research (see methods) to help ensure we isolated CA1sup and CA1deep groups, only including neurons where we had the greatest confidence (Berndt et al., 2023; Mizuseki et al., 2011). In doing so, we excluded neurons which classification was uncertain. It is possible this excludes some meaningful populations of CA1 sublayers. Additionally, despite our approach, some cross-inclusion of sublayers may remain. Therefore, interpretations of CA1 sublayers difference should be considered with these limitations in mind. That said, the number of neurons and animals tested does provide overall confidence regarding our results. Future studies investigating this ACC to CA1 sublayer specific line of communication would benefit from the use of silicon probes or neuropixels that enable precise radial localization.”

> *(5) In the optogenetic experiment in Figure 5, the effect on the CA1 sup neurons seems to be driven by changes in a small subpopulation of this group, with no change in the others. Related to point 2, is there anything else in the data that can pull out what these cells are? More detailed analysis of the firing of these neurons might pull out something really interesting.*

We thank the reviewer for this feedback. Firstly, we want to clarify that optogenetic experiments were performed in a separate cohort of mice that did not undergo contextual fear conditioning. We have adjusted the text accordingly to make this distinction clearer. We have also added a per-animal separation of CA1 heatmap responses to ACC stimulations to demonstrate suppression is preserved across animals (Figure 5—figure supplement 3; Figure 6—figure supplement 2). Finally, our optogenetic experiments were primarily focused on understanding anatomical connectivity. Consequently, common waking behaviors (e.g., exploration and feeding) were not standardized across animals, and our analyses were therefore restricted to comparisons between slow-wave sleep and wakefulness more broadly.

> *(6) Related to this - a number of comparisons simply pool neurons across mice and analyse them as if independent. This is done a lot in the past, but it would be better if an approach that included the interdependence of neurons recorded from the same mouse at the same time were used (such as a hierarchical model). While this is complex, a simpler approach would just be to plot the summary data also per mouse. For example, in Figure 5, how do the neurons inhibited by ACC activation spread across the different mice? Is the level of inhibition related to how well the mice learned the CS-US association?*

For dual-site analysis we have now added animal-level comparison for some key analyses (See Figure—figure supplement 1&2). As for optogenetic experiments, we have added per-animal heatmaps for ACC stimulation response (Figure 5—figure supplement 3; Figure 6—figure supplement 2).

> *(7) Figure 6 is interesting, but very preliminary. None of the effects are quantified, and one of the cell types is not identified. I think some proper analysis needs to be done, again across mice, to be able to draw conclusions from these data.*

We thank the reviewer for this feedback. Reviewer 1 had a similar concern, and we have since added additional analyses to the revisions. Specifically, we performed autocorrelegrams, theta phase modulation analyses and a burst index analysis for V-Type interneurons. Importantly, however, these approaches still collapse neurons across mice.

Given the sparse nature of V-type and PV interneurons, files often contain 2 or fewer interneurons making within-animal comparison difficult. That said, we have added supplemental figures displaying per-animal changes in response to ACC stimulations (Figure 6—figure supplement 1).

> *(8) Finally, in general, I felt that the way the paper was written was very hard to follow, often relying on very processed levels of analysis that were hard to relate back to the raw traces and their biological meaning. In general taking more words to really simply and fully explain each analysis, and taking the words and figures to walk through how each analysis was done and what it tells us about the neuronal data/biology would be really beneficial, especially to someone who is not an extracellular electrophysiologist or immersed in the immediate field.*

We thank the reviewer for this feedback. Throughout the manuscript, we have revised the text to improve clarity in explaining our approaches and their results.

> *In summary, while this manuscript explores an intriguing hypothesis about pre-learning circuit dynamics, it is currently held back by insufficient clarity in behavioural analysis, data presentation, and statistical quantification. Addressing these core issues would greatly improve interpretability and confidence in the findings.*

Additional comment:

For the optogenetic experiments, we reprocessed and resorted the neuronal dataset to ensure accurate cell classification. Following this re-analysis, the principal findings remained unchanged. However, we found that sublayer-specific differences in response to ACC stimulation were restricted to the first second following ACC stimulation. Consequently, we removed the previous Figure 5E, which examined firing rate changes across successive 1-sec time bins, as the additional time windows did not provide further evidence of sublayer-specific effects.

Acsady, L., Halasy, K., & Freund, T. F. (1993). Calretinin is present in non-pyramidal cells of the rat hippocampus--III. Their inputs from the median raphe and medial septal nuclei. Neuroscience, 52(4), 829-841. *https://doi.org/10.1016/0306-4522(93)90532-k*

Andrianova, L., Yanakieva, S., Margetts-Smith, G., Kohli, S., Brady, E. S., Aggleton, J. P., & Craig, M. T. (2023). No evidence from complementary data sources of a direct glutamatergic projection from the mouse anterior cingulate area to the hippocampal formation. eLife, 12, e77364. *https://doi.org/10.7554/eLife.77364*

Behzadi, G., Kalén, P., Parvopassu, F., & Wiklund, L. (1990). Afferents to the median raphe nucleus of the rat: Retrograde cholera toxin and wheat germ conjugated horseradish peroxidase tracing, and selectiveᴅ-[^{3}H]aspartate labelling of possible excitatory amino acid inputs. Neuroscience, 37(1), 77-100. *https://doi.org/10.1016/0306-4522(90)90194-9*

Berndt, M., Trusel, M., Roberts, T. F., Pfeiffer, B. E., & Volk, L. J. (2023). Bidirectional synaptic changes in deep and superficial hippocampal neurons following in vivo activity. Neuron, 111(19), 2984-2994.e2984. *https://doi.org/10.1016/j.neuron.2023.08.014*

Cho, J. H., Deisseroth, K., & Bolshakov, V. Y. (2013). Synaptic encoding of fear extinction in mPFC-amygdala circuits. Neuron, 80(6), 1491-1507. *https://doi.org/10.1016/j.neuron.2013.09.025*

Freund, T. F., Gulyas, A. I., Acsady, L., Gorcs, T., & Toth, K. (1990). Serotonergic control of the hippocampus via local inhibitory interneurons. Proc Natl Acad Sci U S A, 87(21), 8501-8505. *https://doi.org/10.1073/pnas.87.21.8501*

Gulati, T., Guo, L., Ramanathan, D. S., Bodepudi, A., & Ganguly, K. (2017). Neural reactivations during sleep determine network credit assignment. Nat Neurosci, 20(9), 1277-1284. *https://doi.org/10.1038/nn.4601*

Halasy, K., Miettinen, R., Szabat, E., & Freund, T. F. (1992). GABAergic Interneurons are the Major Postsynaptic Targets of Median Raphe Afferents in the Rat Dentate Gyrus. Eur J Neurosci, 4(2), 144-153. *https://doi.org/10.1111/j.1460-9568.1992.tb00861.x*

Huang, W., Ikemoto, S., & Wang, D. V. (2022). Median Raphe Nonserotonergic Neurons Modulate Hippocampal Theta Oscillations. J Neurosci, 42(10), 1987-1998. *https://doi.org/10.1523/JNEUROSCI.1536-21.2022*

Jackson, J., Bland, B. H., & Antle, M. C. (2009). Nonserotonergic projection neurons in the midbrain raphe nuclei contain the vesicular glutamate transporter VGLUT3. Synapse, 63(1), 31-41. *https://doi.org/10.1002/syn.20581*

Liu, Z.-W., Faraguna, U., Cirelli, C., Tononi, G., & Gao, X.-B. (2010). Direct Evidence for Wake-Related Increases and Sleep-Related Decreases in Synaptic Strength in Rodent Cortex. The Journal of Neuroscience, 30(25), 8671. *https://doi.org/10.1523/JNEUROSCI.1409-10.2010*

Miettinen, R., & Freund, T. F. (1992). Convergence and segregation of septal and median raphe inputs onto different subsets of hippocampal inhibitory interneurons. Brain Res, 594(2), 263-272. *https://doi.org/10.1016/0006-8993(92)91133-y*

Mizuseki, K., Diba, K., Pastalkova, E., & Buzsáki, G. (2011). Hippocampal CA1 pyramidal cells form functionally distinct sublayers. Nature Neuroscience, 14(9), 1174-1181. *https://doi.org/10.1038/nn.2894*

Morales, M., & Bloom, F. E. (1997). The 5-HT3 receptor is present in different subpopulations of GABAergic neurons in the rat telencephalon. J Neurosci, 17(9), 3157-3167. *https://doi.org/10.1523/JNEUROSCI.17-09-03157.1997*

Norimoto, H., Makino, K., Gao, M., Shikano, Y., Okamoto, K., Ishikawa, T., Sasaki, T., Hioki, H., Fujisawa, S., & Ikegaya, Y. (2018). Hippocampal ripples down-regulate synapses. Science, 359(6383), 1524-1527. *https://doi.org/10.1126/science.aao0702*

Oh, S. W., Harris, J. A., Ng, L., Winslow, B., Cain, N., Mihalas, S., Wang, Q., Lau, C., Kuan, L., Henry, A. M., Mortrud, M. T., Ouellette, B., Nguyen, T. N., Sorensen, S. A., Slaughterbeck, C. R., Wakeman, W., Li, Y., Feng, D., Ho, A., . . . Zeng, H. (2014). A mesoscale connectome of the mouse brain. Nature, 508(7495), 207-214. *https://doi.org/10.1038/nature13186*

Papp, E. C., Hajos, N., Acsady, L., & Freund, T. F. (1999). Medial septal and median raphe innervation of vasoactive intestinal polypeptide-containing interneurons in the hippocampus. Neuroscience, 90(2), 369-382. *https://doi.org/10.1016/s0306-4522(98)00455-2*

Petreanu, L., Huber, D., Sobczyk, A., & Svoboda, K. (2007). Channelrhodopsin-2–assisted circuit mapping of long-range callosal projections. Nature Neuroscience, 10(5), 663-668. *https://doi.org/10.1038/nn1891*

Rajasethupathy, P., Sankaran, S., Marshel, J. H., Kim, C. K., Ferenczi, E., Lee, S. Y., Berndt, A., Ramakrishnan, C., Jaffe, A., Lo, M., Liston, C., & Deisseroth, K. (2015). Projections from neocortex mediate top-down control of memory retrieval. Nature, 526(7575), 653-659. *https://doi.org/10.1038/nature15389*

Ramanathan, K. R., & Maren, S. (2019). Nucleus reuniens mediates the extinction of contextual fear conditioning. Behavioural brain research, 374, 112114. *https://doi.org/10.1016/j.bbr.2019.112114*

Ramanathan, K. R., Ressler, R. L., Jin, J., & Maren, S. (2018). Nucleus Reuniens Is Required for Encoding and Retrieving Precise, Hippocampal-Dependent Contextual Fear Memories in Rats. The Journal of Neuroscience, 38(46), 9925. *https://doi.org/10.1523/JNEUROSCI.1429-18.2018*

Ratigan, H. C., Krishnan, S., Smith, S., & Sheffield, M. E. J. (2023). A thalamic-hippocampal CA1 signal for contextual fear memory suppression, extinction, and discrimination. Nat Commun, 14(1), 6758. *https://doi.org/10.1038/s41467-023-42429-6*

Senft, R. A., Freret, M. E., Sturrock, N., & Dymecki, S. M. (2021). Neurochemically and Hodologically Distinct Ascending VGLUT3 versus Serotonin Subsystems Comprise the r2-Pet1 Median Raphe. J Neurosci, 41(12), 2581-2600. *https://doi.org/10.1523/JNEUROSCI.1667-20.2021*

Shi, W., Xue, M., Wu, F., Fan, K., Chen, Q. Y., Xu, F., Li, X. H., Bi, G. Q., Lu, J. S., & Zhuo, M. (2022). Whole-brain mapping of efferent projections of the anterior cingulate cortex in adult male mice. Mol Pain, 18, 17448069221094529. *https://doi.org/10.1177/17448069221094529*

Silva, B. A., Astori, S., Burns, A. M., Heiser, H., van den Heuvel, L., Santoni, G., Martinez-Reza, M. F., Sandi, C., & Gräff, J. (2021). A thalamo-amygdalar circuit underlying the extinction of remote fear memories. Nature Neuroscience, 24(7), 964-974. *https://doi.org/10.1038/s41593-021-00856-y*

Souza, R., Bueno, D., Lima, L. B., Muchon, M. J., Gonçalves, L., Donato, J., Jr., Shammah-Lagnado, S. J., & Metzger, M. (2022). Top-down projections of the prefrontal cortex to the ventral tegmental area, laterodorsal tegmental nucleus, and median raphe nucleus. Brain Struct Funct, 227(7), 2465-2487. *https://doi.org/10.1007/s00429-022-02538-2*

Szonyi, A., Mayer, M. I., Cserep, C., Takacs, V. T., Watanabe, M., Freund, T. F., & Nyiri, G. (2016). The ascending median raphe projections are mainly glutamatergic in the mouse forebrain. Brain Struct Funct, 221(2), 735-751. *https://doi.org/10.1007/s00429-014-0935-1*

Tononi, G., & Cirelli, C. (2003). Sleep and synaptic homeostasis: a hypothesis. Brain Research Bulletin, 62(2), 143-150. *https://doi.org/10.1016/j.brainresbull.2003.09.004*

Tononi, G., & Cirelli, C. (2006). Sleep function and synaptic homeostasis. Sleep Med Rev, 10(1), 49-62. *https://doi.org/10.1016/j.smrv.2005.05.002*

Turi, G. F., Li, W. K., Chavlis, S., Pandi, I., O'Hare, J., Priestley, J. B., Grosmark, A. D., Liao, Z., Ladow, M., Zhang, J. F., Zemelman, B. V., Poirazi, P., & Losonczy, A. (2019). Vasoactive Intestinal Polypeptide-Expressing Interneurons in the Hippocampus Support Goal-Oriented Spatial Learning. Neuron, 101(6), 1150-1165 e1158. *https://doi.org/10.1016/j.neuron.2019.01.009*

Wang, D. V., Yau, H.-J., Broker, C. J., Tsou, J.-H., Bonci, A., & Ikemoto, S. (2015). Mesopontine median raphe regulates hippocampal ripple oscillation and memory consolidation. Nature Neuroscience, 18(5), 728-735. *https://doi.org/10.1038/nn.3998*

Wang, J., Hasan, M. T., & Seung, H. S. (2009). Laser-evoked synaptic transmission in cultured hippocampal neurons expressing channelrhodopsin-2 delivered by adeno-associated virus. J Neurosci Methods, 183(2), 165-175. *https://doi.org/10.1016/j.jneumeth.2009.06.024*

Watson, Brendon O., Levenstein, D., Greene, J. P., Gelinas, Jennifer N., & Buzsáki, G. (2016). Network Homeostasis and State Dynamics of Neocortical Sleep. Neuron, 90(4), 839-852. *https://doi.org/10.1016/j.neuron.2016.03.036*

Xu, W., & Südhof, T. C. (2013). A Neural Circuit for Memory Specificity and Generalization. Science, 339(6125), 1290-1295. *https://doi.org/10.1126/science.1229534*

> ***Recommendations for the authors:***
>
> ***Reviewer #1 (Recommendations for the authors):***
>
> *Suggested fixes (these correlate with the numbered points in the Weaknesses section of the Public Review):*
>
> *(1) That seems like the larger finding to start with, before dissecting by Firing Activity Index. I'd first show the overall finding, then dissect it.*

We thank the reviewer for this recommendation. In our manuscript, figure 1F examines the overall pre-to-post prediction gain changes prior to any neuron separation. Further separation of neurons' characteristics and classification occurs in subsequent figures.

> *(2) The overall picture painted by Figure 2 suggests a correlation analysis should be carried out to search for a general property: prediction score gain vs firing activity index. Are those two variables considered significant by Pearson correlation? Did the authors try that and it didn't work, so they did these analyses? If there is no significant correlation, what does a more detailed look at those two variables on an x-y plot teach us? I suggest considering showing such a plot to readers, at least in a Supplement.*

We thank the reviewer for this feedback and have incorporated this approach in our revised manuscript. Specifically, we performed a correlation analysis between prediction gain change and modulation index (formerly called firing activity index). We uncovered a significant positive correlation between variables, suggesting that task engagement modifies ACC→CA1 communication (Figure 2C).

> *(3) (No additional comments).*
>
> *(4) This weakness may be able to be addressed by doing a correlation of depth (LFP amplitude of sharp wave) versus the firing rate ratio. For example, the threshold used for deep may have been such that it reduced the number of detected deep neurons, but if a general relationship between depth and degree of FRR is found, it can remove issues from this difference in statistical power.*

We thank the reviewer for this comment. We were unable to perform a reliable link between correlation depth and modulation index. LFP amplitude can vary substantially between tetrodes due to differences in electrode impedance, placement, and recording conditions, making direct comparisons across animals difficult. While within-animal analyses could largely circumvent these issues, many recording sessions did not include tetrodes spanning the full superficial-to-deep CA1 axis, preventing a reliable assessment of this relationship.

> *(5) I would give it a different name - "opto-modulation index" or "opto firing rate ratio" perhaps. This would make it clear that you are not measuring task-based modulation of firing.*

We have since modified our wording to improve clarity. Specifically, we renamed "Firing Rate Ratio" throughout the manuscript to "Modulation Index". We also relabeled the Figure 5D Y-axis as "Z-scored Firing Response" to more accurately reflect the plotted data and avoid confusion

> *(6) Specifically: can the post-opto lag of v-type versus wide-waveform and PV-type neurons be analyzed? Are the V-type neurons increasing firing before the others decrease? What about cross correlograms between v-type and pyramidal neurons, either at baseline or post-stim?*

We appreciate this feedback. We have added a figure showing differences in response lags to the optostimulation. We demonstrate that V-Type interneurons clearly fire prior to PV and pyramidal cells (Figure 6—figure supplement 1E&F). Additionally, we performed cross-correlogram analyses to examine whether V-type interneurons exhibited consistent temporal relationships with PV interneurons or other CA1 neurons. However, V-type and PV interneurons were sparse throughout our recordings, with most sessions containing two or fewer identified interneurons, which limited our ability to perform meaningful cross-correlation analyses. Nevertheless, we examined the available recordings but found no consistent evidence of correlated firing between interneuron classes or between V-type and pyramidal neurons.

> *(7) Can the authors discuss the candidate pathways for connectivity from ACC to CA1?*

We thank the reviewer for this feedback. We have since added discussions on ACC-to-CA1 connectivity and discussed possible relay brain regions between ACC and CA1.

> *(8) There is mounting evidence about the role of sleep oscillatory events playing homeostatic roles, not only memory-based. The authors bring this up, but do not offer it as an explanation for their findings, but I believe they probably should. For example, Norimoto et al 2018 cited by the authors. Also, Gulati/Gunguly et al 2017 Nature Neuroscience suggests downscaling as a default NonREM activity. Gulati and also Roux/Buzsaki NatNeuro 2017 show that certain privileged or tagged neurons can be protected from this. This therefore reflects that default activity in nonREM may have a homeostatic role, but then learning may alter that default. I believe this should be discussed as a possible reason for the dissociation between ACC and CA1, the authors observe after CFC.*
>
> *In more detail, the authors state that CFC worsened ACC ability to predict ripple spike rate vectors. The authors suggest this may reflect "worsened" communication from ACC to HPC. It could also reflect a SHIFT (not worsening) in the information state of the hippocampus, where ripples reflect novel information and/or information coming from other brain regions. Essentially, the novel information may out-compete usual information flows. For example, ACC may be a default "feeder" into ripples (for example as part of default mode network) when there was no recent highly salient information, but under non-default conditions such as after CFC, ripple content may be fed from other sources (be they internal or external to the HPC). I believe this should be discussed.*
>
> *For example, were CA1 sup task inactive neurons basically DMN-active neurons? Figure 2 shows neurons with the highest pre-training ACC prediction were the ones that dropped the most in training - again suggesting these neurons may be tuned to internal or default dynamics rather than CFC (or other novel experiences).*
>
> *This shift from a default communication mode to a more experience-based one should probably be discussed as an alternative explanation, rather than simply "worsening" of communication.*

We thank the reviewer for this feedback and their recommendation for possible alternate explanations. We have incorporated many of the listed citations and ideas they discussed into our discussion section proposing homeostatic downscaling and a shift in the default mode network as possible explanations for our results.

> *Minor Weaknesses:*
>
> *(1) Introduction Line 52: "during replays" should probably be "during replay events".*

Changed.

> *(2) Introduction Line 76: "how communications" should be "how communication"*

Changed.

> *(3) 200-0, 400-200, 600-400 time bins are a bit unclear in Figure 1f. Are they really negative times, rather than positive? Perhaps negative signs could be put into the legend of 1f, or the time windows can be shown on the left side of 1e. Or potentially 1f could use the same -0.6, -0.4, etc as 1e so readers understand they are linked (if I understand correctly).*

They are negative in the sense the occur before the ripple event. Figure 1e now displays the negative signs.

> *(4) I don't believe the methods describe how many tetrodes are put into the ACC. It would seem this should be put in the ACC portion of the "Stereotaxic surgery" section.*

We now clearly explain the number of tetrodes (8) in the "Stereotaxic surgery" section.

> *(5) Results line 125: "learning induced" should be "learning-induced".*

Changed.

> *(6) In terms of display, deep and sup are swapped in the various figures in terms of which is shown first/second (at least for readers assuming left is first). I suggest putting deep first or sup first in all figures. To me, sup first seems more natural, but homogeneity seems best regardless. This will help readers easily track results.*

We adjusted the figures so that superficial is typically displayed first with some exceptions. For example, in Figure 3A, CA1deep is shown first to preserve the anatomical (dorsal-ventral) relationship.

> *(7) Results line 178: "optogenetics stimulation" should be "optogenetic stimulation".*

Changed.

> *(8) Results line 180: "upon stimulations" should be "upon stimulation".*

Changed.

> *(9) Results line 180: "to different capacities" could be "to different degrees" or "in different manners".*

Changed.

> ***Reviewer #2 (Recommendations for the authors):***
>
> *The sleep scoring procedure is not described clearly. The text references delta waves and ripple oscillations, but the accompanying citation (Wang et al. 2015) does not use such a procedure. Since the post-task rest sessions are called "sleep sessions", there is some confusion about whether the data was restricted to slow wave sleep or not. If data from each sleep session were taken without restricting to actual sleep, that would be problematic because animals may be less likely to sleep immediately following fear conditioning, which could introduce some sleep/wake bias into the comparisons. In particular, the relationship between cortex and ripple activity has been reported to dramatically change between awake and sleep states (Tang & Jadhav, 2019). I am not including this point in the public review in case the data was in fact restricted for sleep, and it simply needs to be clarified in the text.*

Thank you for this feedback. The recordings were in fact restricted to sleep. We have added text to the manuscript to make this clearer. Moreover, we added further discussion on how sleep was calculated.

> *There is a puzzling paragraph in the discussion, arguing that "Here, we add to this understanding with CA1sup neurons having a diminished role in fear memory formation". Sparse task-related activity in CA1sup does not imply that CA1sup is not involved in memory. Indeed, while the median of CA1sup neurons' firing rate ratio was below zero, there is a substantial proportion of neurons that are recruited, and these could be extremely important for memory. Most studies on reactivation and replay would only concentrate on cells sufficiently active in the task, and observe whether these patterns of activity are enhanced in post-task sleep.*

We thank the reviewer for this feedback and have removed the text claiming sublayer difference in fear conditioning.

> *If the ACC is indeed inhibiting the CA1sup pyramidal cells through V-type interneurons, then one would expect the average GLM weights predicting the activity of those best-predicted CA1sup cells to be negative. If that is true, that could nicely tie the prediction effect to the optogenetic results, demonstrating that ACC's relationship to pyramidal cells is inhibitory in natural conditions as well.*

We thank the reviewer for this suggestion. Unfortunately, our primary GLM analysis did not properly save weight coefficients to perform such analyses. To address this as closely as possible, we performed a preliminary analysis using a modified version of our GLM to examine whether the coefficients predicting CA1sup pyramidal neuron activity exhibited a bias toward negative weights. While this modified analysis did not generate coefficients directly comparable to the prediction gain values reported in the manuscript, it allowed us to assess whether an overall difference in coefficient sign was evident between CA1 sublayers. We found no significant bias toward negative coefficients and no clear differences between CA1sup and CA1deep neurons. Although this result does not provide additional support for an inhibitory relationship under natural conditions, it does not necessarily contradict our optogenetic findings. GLM coefficients quantify statistical dependencies between neural activities and reflect not only direct interactions but also indirect network effects, shared inputs, and the model structure. Consequently, the sign of a GLM coefficient should not be interpreted as a direct measure of whether the underlying synaptic relationship is excitatory or inhibitory.

> *Figure 1f is strangely missing comparisons for positive delays. If such windows were to be included and if the reactivation gain is lower for them, that could really drive home the point that communication takes place in the ACC->CA1 direction more than in the CA1->ACC direction.*

Our goal of this study was to examine how incoming information from the cortex may differentially drive CA1 sublayer activity. While we think examining the reverse direction offers a compelling future direction, it was beyond the scope of our present manuscript.

> *There is some confusion about the N-s. There's a total of 190 CA1 neurons (Figure 2a legend). 21 of them are deep, and 77 are sup (Figure 3b legend), so presumably 92 would be neither. The legend of Figure 4b agrees with this: 24 task-active CA1sup and 53 task-inactive CA1sup cells, while in CA1deep, there were 14 task-active and 7 task-inactive cells, but in Figure 3c, there is a comparison of N=24 CA1deep cells and n=94 CA1sup cells (so 72 neither).*

For one dual-site animal, the CFC recording file was corrupted, while the pre- and post-training recordings remained intact. As a result, this animal was included only in the GLM

analyses, leading to slight differences in sample size across analyses. We have clarified these sample sizes in the revised manuscript and highlighted this discrepancy in the Methods section.

> *There appears to be a typo on line 213, the reference should be to Figure 6f.*

Changed.

> ***Reviewer #3 (Recommendations for the authors):***
>
> *To what extent do the authors think that this is learning dependent, as opposed to stress dependent? Not that I want an experiment here, but it is important to note that both of these regions are very much involved in stress responses. Do you think you would get the same result with a purely appetitive learning paradigm? Or is this specific to stress? It might be nice to add this to the discussion.*

We thank the reviewer for this raising this point of discussion. Future experiments utilizing appetitive behavioral tasks could help address these important questions. While we have avoided speculating too much, we agree it is valuable to acknowledge this possibility. Accordingly, we have added a brief discussion point to at least call attention to this possibility for the reader.

"Another caveat to mention is that both the ACC and CA1 are involved in the stress response (Kim et al., 2015; Lamotte et al., 2021). Future experiments utilizing appetitive learning paradigms, rather than the aversive contextual fear conditioning used here, will help disentangle learning-related remodeling of ACC→CA1 communication from changes driven by stress."

> *There are a number of typos that confuse the message - for example, in the abstract, the authors say that ACC suppresses superficial CA1 interneurons. This seems most likely an error - I think the authors mean superficial CA1 neurons? Or PV interneurons? Similar errors exist throughout, as well as odd combinations of bold and italics across and within words, etc. Overall, especially in consideration of my final main point above regarding clarity of the text, it would be good to have a proper proofread to make sure the text is as clear as possible*

We thank the reviewer for identifying these issues. The specific error in the abstract has been corrected, and we have since carefully proofread the revised manuscript.

https://doi.org/10.7554/eLife.107370.2.sa0